Fracture Repair in *Cyp24a1* Deficient Mice: Biomechanical Properties of Repaired Bones and Contribution to Mechanisms Involved

Bachar Nadim Hamade, M.D.

Division of Surgical Research

McGill University, Montreal, Quebec, Canada

July 2013

A thesis submitted to McGill University in partial fulfillment of the requirements of the degree of Master of Science in Experimental Surgery

To my Parents,

Brothers and Sister

Table of Contents

Abstract 4

Résumé 6

Acknowledgments 8

List of Abbreviations 10

List of Figures 12

List of Tables 13

1. Background Information 14
   - 1.1 Vitamins 14
   - 1.2 Vitamin D-dependent Rickets 23
   - 1.3 CYP24A1 and 24,25-$(OH)_2$D 27
   - 1.4 Engineering the Cyp24a1 Gene Deficient Mouse 32
   - 1.5 Identifying a Receptor for 24,25-$(OH)_2$D 35
   - 1.6 Fracture Repair 38
   - 1.7 Intamedullary Nails 40
   - 1.8 Bone Biomechanics 42
2. Aims of the Study 46
   - 2.1 mRNA and Protein Expression 46
   - 2.2 Biomechanical Testing 46
3. Original Contributions to the Aims 46
4. Materials and Methods 47
   - 4.1 mRNA Quantification 47
   - 4.2 Protein Expression 49
   - 4.3 Immunohistofluorescence 52
   - 4.4 Surgical Experimental Design 55
   - 4.5 Statistical Analysis 61
5. Results 61
   - 5.1 FAM57B 61
   - 5.2 Intramedullary Nailing Experiment 70
6. Discussion 76
7. References 84

Abstract

Vitamin D is a key modulator and regulator of mineral and bone homeostasis. The main active form of vitamin D in the body is the 1,25-$(OH)_2$D metabolite that is formed in the kidney from 25-(OH)D by the enzyme CYP27B1. The enzyme CYP24A1 initiates the C24-oxidation pathway that leads to degradation of the hormonal form of vitamin D, but is also responsible for the synthesis of 24,25-$(OH)_2$D. The putative biological activity of 24,25-$(OH)_2$D remains unclear, but it has been found that following tibial fractures in chicks, the levels of CYP24A1 activity and serum 24,25-$(OH)_2$D are both elevated. Our laboratory has engineered a mouse deficient for the *Cyp24a1* gene to study the role of 24,25-$(OH)_2$D, and has identified a putative membrane receptor (FAM57Bv2) to 24,25-$(OH)_2$D. In this study we assessed the biomechanical properties (stiffness and force needed to break) of the repaired bones of mutant and wild-type mice at different intervals in the presence or absence of treatment with exogenous 24,25-$(OH)_2$D. We also assessed the mRNA and protein expression of the putative receptor in different organ tissues of wild-type mice. Methods: wild-type and *Cyp24a1*-deficient mice were subjected to a modified open osteotomy with subsequent intramedullary nailing of the tibia, followed by subcutaneous treatment with vehicle (propylene glycol) or 6.7 μg/kg of 24,25-$(OH)_2$D. Tibiae were collected on days 18 and 28 post operatively, and the biomechanical properties were tested using a three point bending testing machine. To assess the mRNA and protein expression of *Fam5bv2* in different tissues, qRT-PCR, western blot analysis and immunohistofluorescence were performed. Results: at day 18, we observed significantly inferior biomechanical parameters in the male and female mutant mice injected with vehicle compared to their wild-type littermates. These differences were rescued by exogenous administration of 24,25-$(OH)_2$D. No statistically significant differences were measured at day 28. qRT-PCR analysis showed high mRNA expression of *Fam57bv2* in skin and cartilage, while western blot analysis showed FAM57B (all isoforms) to be expressed in all tissues studied. Immunohistofluorescence studies showed detection of FAM57B in brain paraffin sections, and kidney and tibial

cryosections. Conclusion: The results of this study confirm the delay of fracture healing in *Cyp24a1*-deficient mice and support a role for 24,25-$(OH)_2$D in optimizing fracture healing. Our expression monitoring results show that the putative receptor for 24,25-$(OH)_2$D, FAM57Bv2, is broadly expressed with enrichment in chondrocytes, which may contribute to improved fracture healing.

Résumé

La vitamine D est un modulateur clé de l'homéostasie des minéraux. La forme active de la vitamine D est la 1,25-$(OH)_2$D synthétisée au niveau du rein par l'action de l'enzyme CYP27B1 sur le précurseur 25-(OH)D. L'enzyme CYP24A1 initie la voie d'oxydation C24 qui conduit à la dégradation de la forme hormonale de la vitamine D, mais est également responsable de la synthèse de 24,25-$(OH)_2$D. L'activité biologique de la 24,25-$(OH)_2$D demeure controversée, mais il a été constaté qu'à la suite de fractures du tibia chez les poussins, les niveaux d'activité de la CYP24A1 et les niveaux sériques de 24,25-$(OH)_2$D sont stimulés. Notre laboratoire a mis au point une lignée de souris déficientes pour le gène *Cyp24a1* afin d'étudier le rôle de la 24,25-$(OH)_2$D, et a identifié une molécule qui pourrait agir comme récepteur membranaire pour la 24,25-$(OH)_2$D (FAM57B2). Dans cette étude, nous avons évalué les propriétés biomécaniques (rigidité et la force maximale pour rompre) des os réparés chez des souris mutantes et de type sauvage, suite à un traitement en présence ou absence de 24,25-$(OH)_2$D exogène. Nous avons également évalué l'expression de l'ARNm et de la protéine du récepteur putatif dans différents organes chez les souris sauvage. Méthodes: les souris de type sauvage ou déficiente pour le gène *Cyp24a1* ont été soumise à une ostéotomie ouverte modifiée du tibia avec insertion d'un clou médullaire, suivie d'un traitement sous-cutané avec le véhicule (propylène glycol) ou avec 6,7 µg/kg de 24,25-$(OH)_2$D. Les tibias ont été prélevés aux jours 18 et 28 suivant la chirurgie, et les propriétés biomécaniques ont été testées en utilisant un test de flexion à trois points. Pour évaluer l'ARNm et l'expression de la protéine de *Fam57bv2* dans différents tissus, une amplification par PCR quantitative, l'immunobuvardage et l'immunohistofluorescence ont été utilisés. Résultats: au jour 18, nous avons observé que les paramètres biomécaniques sont nettement inférieurs chez les souris mutantes mâles et femelles injectées avec le véhicule par rapport aux animaux de type sauvage. Ces différences disparaissent suite à l'administration de 24,25-$(OH)_2$D exogène. Aucune différence statistiquement significative n'a été mesurée au jour 28. L'analyse qRT-PCR a montré une expression elevée de l'ARNm de *Fam57bv2* dans la peau et le cartilage, tandis

que l'analyse par immunobuvardage a montré que FAM57B (toutes les isoformes) est exprimée dans tous les tissus étudiés. L'immunohistofluorescence a permis de détecter FAM57B dans des coupes en paraffine de cerveau et dans des cryosections de rein et de tibia. Conclusion: Les résultats de cette étude confirment le retard de la guérison des fractures chez les souris déficientes en *Cyp24a1* et soutiennent un rôle de la 24,25-$(OH)_2$D à optimiser la guérison des fractures. Nos résultats concernant l'expression de FAM57B montrent que le récepteur potentiel de la 24,25-$(OH)_2$D, FAM57Bv2, est exprimé à des niveaux élevés dans les chondrocytes, ce qui appuie une contribution mécanistique au cours de la guérison des fractures.

Acknowledgments

First and foremost, I would like to thank my supervisor, Dr. René St-Arnaud, for his excellent mentorship, guidance, availability, and constant support. I had the privilege of having Dr. St-Arnaud as my supervisor over the past two years; he always maintained a professional yet pleasurable environment in the laboratory and was readily available to give his valuable input on my work. I was very fortunate to have him as my supervisor and I would like to greatly thank him for the opportunity he gave me in pursuing my Masters degree. Thank you René.

I would also like to thank a former Masters student and a dear friend of mine, Abdallah Husseini, for taking the time and effort in teaching me his intramedullary nailing technique. He was always available for questions and guidance and was truly a key player in my learning curve.

Great thanks go to all my research laboratory colleagues, Alice Arabian, László Kupcsik, Martin Pellicelli, Bahareh Hekmatnejad and Toghrul Jafarov for training me and teaching me the various techniques used in my project. I would also like to thank them for making me feel part of the family over the past two years, and in maintaining the most pleasurable environment possible. In addition I would like to thank Waleed Al Bishi, a colleague and a dear friend for his constant support and his unwavering cheerful attitude throughout my stay.

A special acknowledgement goes to the members of the Shriners animal facility, Mia Esser, Nathalie Girard, and Louise Marineau, for breeding and maintaining my mice, and their assistance in collecting my samples.

I have been very fortunate in my life to have been blessed with great friends; listing the names would run endlessly but some have truly made a huge impact on my life and deserve to be mentioned. Very special thanks go to, Elie Alam, Omar

El Ayach, Zaid Diken, Grace Hayek, Aline Zouk, Grace Salame, Makram Mickey Hamade, Bassel El-Koussa, Fawzi Saoud, Ghady Haidar, Robert Frangie, Marc Mourad, Rami Awada, Hisham Zebian, Andréa Geara, Natasha Couvrette, Marylana Saadeh and Hiba Sabra for being amazing friends and more, who have each in their own special way helped me and supported me in pursuing my dreams. You have always been there for me and for that I thank you from the bottom of my heart.

In the end, words cannot describe my utmost gratitude and thanks to my parents, Nadim and Ahlam, my brothers, Firas and Tarek, and my sister Diala. Their unconditional love, unwavering support and belief in me have been my driving force all my life. Without them I would have not been able to get to where I am today, and for that I am forever grateful. Thank you for being the most loving parents, the best brothers and friends, and the most amazing and caring sister ever. You're more than I could have ever wished for. Thank you for everything.

List of Abbreviations

BSA	Bovine serum albumin
Calcitriol	1,25-$(OH)_2D$
CaSR	Calcium sensing receptor
cDNA	Complimentary deoxyribonucleic acid
COS-7	CV-1 Origin, SV40 transformed monkey kidney fibroblast-like cells
CYP24A1	1,25-dihydroxyvitamin D_3-24-hydroxylase
CYP27A1	Mitochondrial vitamin D_3-25-hydroxylase
CYP27B1	25-hydroxy vitamin D-1-α-hydroxylase
CYP2R1	Microsomal vitamin D_3-25-hydroxylase
DBP	Vitamin D binding protein
DNA	Deoxyribonucleic acid
ELISA	Enzyme-linked immunosorbent assay
FAM57B	Family with sequence similarity 57 member B
FAM57Bv2	Family with sequence similarity 57 member B isoform 2
FGF23	Fibroblast growth factor 23
GAPDH	Glyceraldehyde 3-phosphate dehydrogenase
HVDRR	Hereditary Vitamin-D-Resistant Rickets
IHF	Immunohistofluorescence
IM	Intramedullary
MC3T3-E1	Mouse calvaria preosteoblasts isolated via the 3T3 protocol
micro-CT	Micro computed tomography
mRNA	Messenger ribosomal nucleic acid
OCT	Formulation of water-soluble glycols and resins
PBS	Phosphate-buffered saline
PCR	Polymerase chain reaction
PDDR	Pseudo vitamin D deficiency Rickets
PTH	Parathyroid Hormone
qRT-PCR	quantitative Real-time reverse transcription polymerase chain reaction
RANK	Receptor activator of nuclear factor-κB
RANKL	Receptor activator of nuclear factor-κB ligand
RCF	Relative centrifugal force
RIPA	Radio immune precipitation assay
RNA	Ribonucleic acid
RPM	Rounds per minute
RXR	Retinoid X receptor

TBS	Tris-buffered saline
TRPV5	Transient receptor potential cation channel, subfamily V, member 5
TRPV6	Transient receptor potential cation channel, subfamily V, member 6
VDDR	Vitamin D-dependent Rickets
VDR	Vitamin D receptor
WT	Wild-type

List of Figures

Figure 1: Radiograph of Osteomalacia and Rickets

Figure 2: The two forms of vitamin D

Figure 3: Synthesis and activation of vitamin D

Figure 4: Regulation of CYP27B1

Figure 5: Actions of 1,25-$(OH)_2$D

Figure 6: Degradation of 1,25-$(OH)_2$D by CYP24A1

Figure 7: Inactivation of *Cyp24a1*

Figure 8: Impaired vitamin D catabolism in *Cyp24a1*$^{-/-}$ mice

Figure 9: BV/TV comparison between wild-type and mutant mice calluses

Figure 10: Binding of 24,25-$(OH)_2$D to FAM57B

Figure 11: Image of locking nail

Figure 12: Stress-strain curve

Figure 13: Steps of the surgical procedure

Figure 14: Postoperative radiograph image

Figure 15: Image of three-point bending procedure

Figure 16: qRT-PCR of *Fam57b* and *Fam57bv2* for WT mice

Figure 17: Western blot analysis of FAM57B

Figure 18: Brain paraffin sections

Figure 19: Kidney cryosections

Figure 20: Tibia cryosections

Figure 21: Male three-point bending results at day 18 post-operation

Figure 22: Female three-point bending results at day 18 post-operation

Figure 23: Male three-point bending results at day 28 post-operation

Figure 24: Female three-point bending results at day 28 post-operation

List of Tables

Table 1: Clinical manifestations of PDDR and Vitamin D deficiency rickets

Table 2: Comparison of 1α-Hydroxylase deficiency and HVDRR

Table 3: *Cyp24a1*$^{-/-}$ mice survival percentage

1. Background Information

1.1 Vitamins

By the end of the 19th century and with the beginning of the 20th century, the field of nutrition and its original views on what was considered to be a normal adequate diet capable of sustaining growth and development began to change. Reports in the field began to reveal that there might be micro organic nutrients present in natural foods, that were essential for growth and the prevention of certain diseases (Deluca, 2011). Feeding inmates with whole rice instead of polished rice eliminated the neurological disease Beri-Beri (Eijkman, 1897), and the consumption of limes by sailors prevented the development of scurvy (Holst et al., 1907). It was eventually reasoned that processed foods lacked the "vital amines" found in natural foods that were essential for normal growth and development and the prevention of disease; these were then termed "vitamins" (Funk, 1911).

1.1.1 Vitamin D

Vitamin D belongs to the family of fat-soluble vitamins that the body requires to function properly. The discovery of Vitamins A and B (McCollum et al., 1916) paved the way for its discovery and its addition to the family of vitamins; at the time, researchers thought that cod liver oil (a source rich in vitamin A) had the ability to cure Rickets. When it was discovered that the component present in cod liver oil curing Rickets was not vitamin A, it was called vitamin D. In reality Vitamin D is not an actual vitamin but a pre-hormone that requires multiple steps of modification in the body before becoming active and exerting its effects. Thus naming it vitamin D was in fact a mistake, however, this nomenclature persists and is still widely used today (Deluca, 2011).

1.1.2 Historical Background on Vitamin D

With the industrial revolution at the end of the 19th century, the prevalence of Rickets was increasing especially in low-sunlight countries such as England (Deluca, 2011). Rickets is a disease of children, whereas osteomalacia is a disease of the adults. During childhood, defective mineralization of the osteoid (unmineralized bone) is mostly evident at the growing ends of bones, and this leads to widening of the growth plate and expansion in the width of the adjacent metaphysis. With progression of the disease, the changes become more and more apparent at sites of bone which are growing most actively such as the knee, wrists, ribs and many others, eventually leading to the skeletal deformities characteristic of the disease (**Figure 1A**). In adults, longitudinal bone growth ceases due to the fusion of the epiphysis to the metaphysis, but bone turnover continues throughout life. Therefore, unmineralized osteoid in adults accumulates in sites other than the growth plate resulting in a condition termed osteomalacia (**Figure 1B**) (Adams, 2011).

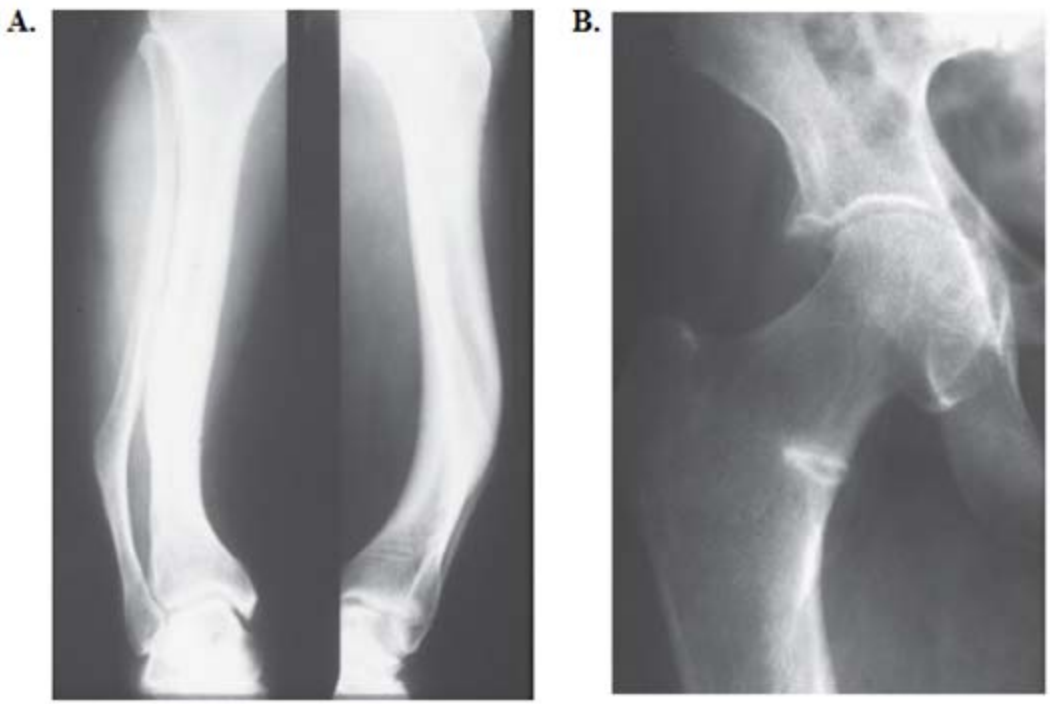

Figure 1: A. Bowing of the tibia and fibula in a child with rickets. **B.** AP radiograph of right hip of patient with osteomalacia revealing Looser's zones. These are radiolucent lines perpendicular to the cortex with sclerotic margins that are significant of unmineralized osteoid. Taken from (Adams, 2011).

After the discovery of vitamins A and B, it was reasoned that rickets might also be caused by a dietary deficiency. Dogs maintained on a diet composed mainly of oatmeal eventually developed rickets, but were healed when supplemented with cod liver oil. Thus the reversal and prevention of rickets were first attributed to vitamin A (Mellanby, 1989); but when cod liver oil was treated in a manner resulting in the destruction of vitamin A, the healing effects were not lost and therefore the nutrient behind this phenomenon was an unknown vitamin that was then labeled vitamin D (McCollum et al., 1922). At the same time, another group was able to show that exposing children to sunlight or artificial ultraviolet light was able to cure or prevent rickets (Chick, 1976), and that in fact ultraviolet light was able to activate an inactive substance to become a vitamin-D-active material (Steenbock et al., 1925).

In the 1930s, the nutritional forms of vitamin D were finally isolated and identified. The two forms, vitamin D_2 and vitamin D_3 differ slightly in chemical structure (**Figure 2**), but this does not alter their function and metabolism in the body (St-Arnaud et al., 2012). Vitamin D_2 is known as ergocalciferol and was identified and isolated from plant sterol irradiation experiments (Askew et al., 1930), while vitamin D_3 which is known as cholecalciferol, was identified and isolated from the skin after the transformation of 7-dehydrocholesterol by sunlight irradiation (Windaus et al., 1936). In this work, we will concentrate on vitamin D_3 and will simply refer to it from here on as vitamin D.

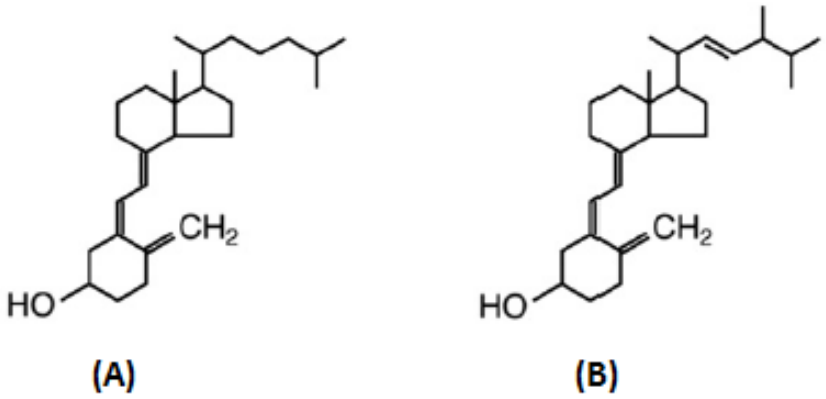

Figure 2: A. Vitamin D_3 (Cholecalciferol). **B.** Vitamin D_2 (Ergocalciferol). Ergocalciferol contains a double bond between C-22 and C-23, as well as a CH_3 group on C-24. These chemical differences do not alter function in the body. Taken from (St-Arnaud et al., 2012).

1.1.3 Vitamin D: Form, Synthesis and Activation

As stated above, before vitamin D can exert any of its biological effects in the body, it needs to undergo a series of biochemical modifications that involve multiple enzymes present in the skin, liver and the kidney. Around 80% of vitamin D requirements in humans are attainable from the skin upon exposure to sunlight, while the rest are obtained from dietary intake (fish, plants and grains) (St-Arnaud et al., 2012). The first step begins with the transformation of 7-dehydrocholesterol in the skin under the effect of ultraviolet light into pre-vitamin D which rapidly transforms into the more thermodynamically stable vitamin D

(Holick, 2011). This molecule then leaves the skin and enters the circulation bound to the vitamin D binding protein (DBP) and is transported to the liver to undergo hydroxylation at carbon number 25 resulting in 25-(OH)D (St-Arnaud et al., 2012). Two enzymes are responsible for this hydroxylation step: CYP2R1 and CYP27A1. These enzymes, as all vitamin D hydroxylases, belong to the super family of cytochrome P450 enzymes. It is suggested that CYP2R1 is the more physiologically relevant enzyme of the two; it is a liver microsomal high-affinity, low capacity enzyme whose discovery was fairly recent (Cheng et al., 2003). On the other hand, CYP27A1 is a liver mitochondrial low-affinity, high capacity enzyme (Cali et al., 1991) whose physiological relevance has always been debatable (St-Arnaud et al., 2012). Patients with inherited cerebrotendinous xanthomatosis caused by a mutation in *CYP27A1* have no obvious defects in vitamin D metabolism, and have normal levels of 25-(OH)D and 1,25-$(OH)_2$D in the circulation (Kuriyama et al., 1993). It is now reasoned that CYP2R1 is the physiologically relevant enzyme at normal vitamin D concentrations, and that CYP27A1 backs it up when concentrations rise into the pharmacological range (St-Arnaud et al., 2012).

The major circulating form of vitamin D in the body is 25-(OH)D; the serum level of this metabolite is reflective of vitamin D status in the body (Holick, 2007). It is now known that adequate circulating levels of 25-(OH)D are critical for overall health maintenance and proper function of the immune, reproductive and musculoskeletal systems of both genders (Holick et al., 2008). The most recent lower and upper limits of normal circulating levels of 25-(OH)D that were agreed upon to avoid heath problems and adverse effects were 20 and 50 ng/ml respectively (Ross et al., 2011; Rosen et al., 2012).

From the liver, 25-(OH)D travels to the kidney where it is hydroxylated at carbon number 1 by the enzyme 25-hydroxyvitamin D-1α-hydroxylase (CYP27B1). This hydroxylation step takes place mainly in the proximal convoluted tubule (Yamagata et al., 2001) and results in 1,25-$(OH)_2$D (calcitriol) which is considered to be the main active form of vitamin D (Omdahl et al., 2002). Only

after interaction with the nuclear vitamin D receptor (VDR) is 1,25-$(OH)_2$D able to carry out its function in the body (**Figure 3**) (Haussler et al., 1998).

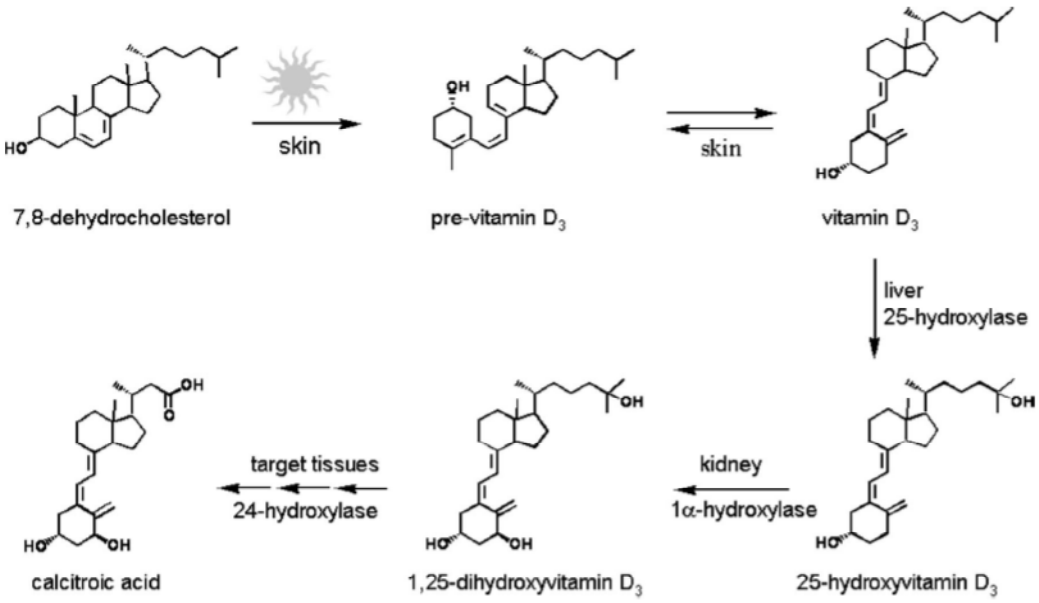

Figure 3: The hydroxylation process of vitamin D. 7-dehydrocholesterol is transformed into pre-vitamin D_3 under the effect of UV light, and rapidly becomes the more stable vitamin D_3. Vitamin D_3 then travels to the liver and is hydroxylated at carbon number 25 by CYP2R1 and CYP27A1 becoming 25-(OH)D. This molecule then travels to the kidney where it becomes 1,25-$(OH)_2$D after hydroxylation at carbon number 1 by CYP27B1. 1,25-$(OH)_2$D is finally metabolized and degraded by a series of enzymatic reactions into calcitroic acid and excreted from the body. Taken from (Dusso et al., 2005).

1.1.4 Role of 1,25-$(OH)_2$D in Bone Health and Mineral Ion Homeostasis

The biological actions of vitamin D in the body are not achieved unless its active form 1,25-$(OH)_2$D binds to the VDR (Haussler et al., 1998). This active metabolite has been shown to have great effects on many systems but most importantly the skeletal system (Omdahl et al., 2002). In this work we will only focus on its role in the skeletal system and particularly mineral ion homeostasis and bone health.

The main role of 1,25-$(OH)_2D$ is to help maintain calcium and phosphate homeostasis through different mechanisms in the body (Haussler et al., 1998; Heaney, 2011), and thus the expression of the *CYP27B1* gene in the kidney is subjected to tight regulation by an interplay of multiple positive and negative feedback loops that involve the parathyroid hormone (PTH), calcitonin, fibroblast growth factor 23 (FGF23), calcium, phosphorus and 1,25-$(OH)_2D$ (**Figure 4**) (Henry, 2011; St-Arnaud et al., 2012).

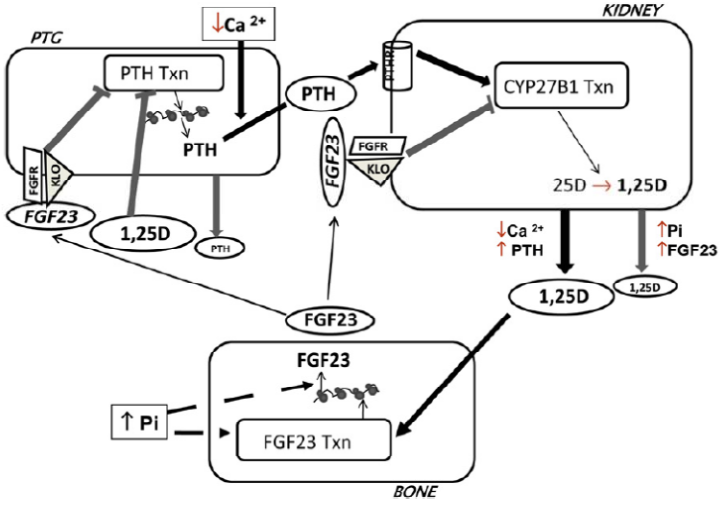

Figure 4: Hormones that regulate the activity of CYP27B1 (1α-hydroxylase) in the kidney. (Top left): A drop in serum calcium levels stimulates the release of PTH from the parathyroid gland, which in turn increases *CYP27B1* activity in the kidney; 1,25-$(OH)_2D$ also acts in a negative feedback loop on its own synthesis by decreasing the synthesis and secretion of PTH. (Top right): A drop in calcium increases the secretion of 1,25-$(OH)_2D$ from the kidney; 1,25-$(OH)_2D$ increases the expression of FGF23 in the bone which has an inhibitory effect on *CYP27B1* activity in the kidney. (Bottom): Elevated phosphate levels increase the production of FGF23 in the bone which inhibits CYP27B1 synthesis in the kidney and PTH transcription in the parathyroid glands. Taken from (Henry, 2011).

The calcium sensing receptors (CaSR) are found in the chief cells of the parathyroid gland, thyroid C-cells and cells of the renal tubules; their main function is to detect a drop in serum calcium levels below normal leading to a release in PTH (Onyango et al., 1999; Pallais et al., 2004). Any inactivating

mutations in the gene coding for the CaSR will result in inappropriate secretion of PTH in the presence of hypercalcemia and hypocalciuria with resultant hypercalcemic adverse effects, as seen in Familial Hypocalciuric Hypercalcemia (Attie et al., 1983; Hebert et al., 1997). This PTH release upregulates the activity of CYP27B1 in the kidney resulting in a production increase of 1,25-$(OH)_2$D to increase calcium absorption in the intestine (Favus et al., 1974; Heaney, 2011; Henry, 2011), by binding to VDR in the intestinal lumen cells; VDR is the only known nuclear receptor that binds this metabolite with high affinity (Haussler et al., 1988), around three orders of magnitude higher than that for 25-(OH)D (St-Arnaud et al., 2012).

VDR is encoded by the *VDR* gene and is expressed in most mammalian tissues (Carlberg et al., 2007) such as the intestine, liver, muscle, kidney and bone (Norman, 1998). It belongs to the subfamily of nuclear hormone receptors which also includes the retinoic acid receptors, retinoid X receptors and thyroid hormone receptors. Each of these three members of the subfamily is known to have more than one characterized isoform (α, β, γ), surprisingly only one form of VDR has been isolated. The DNA binding domain is comprised of two zinc fingers and is found in the very short N-terminus; this domain has also been shown to have a role in nuclear localization and contributes to heterodimerization. Binding of 1,25-$(OH)_2$D occurs in the C-terminus of VDR that also plays a role in heterodimerization and interaction with other nuclear receptor co-activators. Upon interaction of the ligand with VDR, a heterodimer is formed with the retinoid X receptor (RXR) that binds to target genes in target cells to regulate their transcription with the help of nuclear receptor co-activators (Haussler et al., 1998; St-Arnaud et al., 2012).

The activation of VDR by 1,25-$(OH)_2$D in the intestinal lumen cell causes an increase in calcium and phosphate absorption to regulate mineral ion homeostasis (**Figure 5**) (Haussler et al., 1998; Heaney, 2011). The underlying mechanism of the increase in calcium absorption is through the upregulation of a specific calcium channel known as transient receptor potential cation channel, subfamily

V, member 6 (TRPV6) (Holick, 2007), whereas the upregulation of the sodium-phosphorus co-transporter (NaPi-IIb) allows for intestinal phosphorus reabsorption (Xu et al., 2002). Similarly, a channel called transient receptor potential cation channel, subfamily V, member 5 (TRPV5) is present in the distal tubules of the kidney. The activation of VDR in the kidney by 1,25-$(OH)_2$D upregulates the expression of this channel resulting in an increase in calcium reabsorption (Hoenderop et al., 2003).

To further regulate calcium and phosphate homeostasis, 1,25-$(OH)_2$D binds to VDR in osteoblasts and results in the increased expression of the receptor activator of nuclear factor-κB ligand (RANKL) which then binds to its receptor RANK on preosteoclasts. This induces the maturation of the preosteoclasts into mature osteoclasts that act on bone to mobilize calcium and phosphorus to further regulate homeostasis (**Figure 5**) (Holick, 2007).

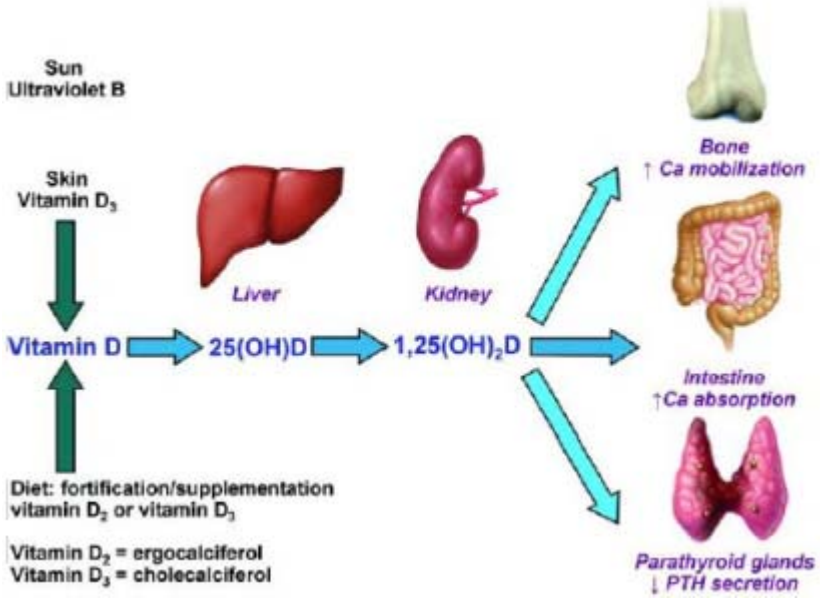

Figure 5: 1,25-$(OH)_2$D regulates calcium homeostasis by increasing intestinal calcium absorption and by increasing calcium mobilization from bone. Taken from (Thacher et al., 2011).

We have described above the role of the CYP27B1 enzyme and calcitriol in maintaining calcium and phosphate mineral ion homeostasis. The identification of two autosomal recessive genetic disorders that cause rickets in children, have further showed the crucial importance of this enzyme and its product. Advances in technology and science have allowed researchers to engineer mouse models representative of these diseases to further provide insight on the importance of CYP27B1, calcitriol, and the VDR (Malloy et al., 2010).

1.2 Vitamin D-dependent Rickets

1.2.1 Vitamin D-dependent Rickets Type I (VDDR I): Pseudo vitamin D Deficiency Rickets (PDDR)

In 1997, several groups were successful in cloning *CYP27B1* (Fu et al., 1997; Monkawa et al., 1997; Shinki et al., 1997; St-Arnaud et al., 1997; Takeyama et al., 1997). It was not until then that the previous hypothesis of vitamin D-dependent rickets type I (VDDR I) being the result of a defective conversion of 25-(OH)D to 1,25-$(OH)_2$D (Fraser et al., 1973) was validated, and that VDDR I was in fact caused by mutations in *CYP27B1* (Fu et al., 1997). The name pseudo vitamin D deficiency rickets (PDDR) stems from the notion that these patients have very low values of 1,25-$(OH)_2$D which might mislead a physician into thinking that this is a mere case of vitamin D deficiency rickets (Prader et al., 1961). Clinical manifestations of PDDR usually appear within the first year of life and are a bit different than classic manifestations of vitamin D deficiency rickets (**Table 1**). These patients present with hypotonia, delayed gross motor development, growth retardation, hypocalcemic seizures, fractures and classic radiographical findings of rickets (Glorieux et al., 2011). Laboratory analysis typically show hypocalcemia, hypophosphatemia, secondary hyperparathyroidism, increased alkaline phosphatase, and almost undetectable levels of 1,25-$(OH)_2$D despite normal 25-(OH)D levels (Malloy et al., 2010; Glorieux et al., 2011). These patients do not respond to treatment with

cholecalciferol (Malloy et al., 2010), but their condition is reversed within less than a year after treatment with calcitriol (**Table 2**) (Delvin et al., 1981; Malloy et al., 2010). The successful inactivation of *Cyp27b1* in mice created a murine model that mimicked PDDR and was able to add more insight to the disease. Indeed, the skeletal and biochemical abnormalities in these mice were not different from what was described previously in PDDR patients (Dardenne et al., 2001; Panda et al., 2001). Surprisingly, the hypocalcemia was normalized when these mice were maintained on a high calcium, phosphorus, and lactose diet, but despite this interesting observation, it was concluded that this normalization cannot substitute for vitamin D action in skeletal homeostasis and that both are required to maintain normal osteoblastic and osteoclastic function (Goltzman et al., 2004; Panda et al., 2004).

Table 1: Differences in clinical manifestations between PDDR and vitamin D deficiency rickets. Taken from reference (Glorieux et al., 2011).

	PDDR	**Vitamin D deficiency rickets**
Short stature	70%	3%
Motor delay	70%	3%
Seizures	15%	25%
Clinical signs of rickets	100%	70%

1.2.2 Vitamin D-dependent Rickets Type I (VDDR II): Hereditary Vitamin-D-Resistant Rickets (HVDRR)

The second genetic autosomal recessive disorder is known as hereditary vitamin D-resistant rickets (HVDRR). The underlying cause of this disease is a loss of function mutation in VDR rendering it partially or completely resistant to 1,25-$(OH)_2$D (Malloy et al., 2011). The clinical manifestations of this disease are quite similar to PDDR with the exception of total or partial alopecia seen in some HVDRR patients. Biochemically these patients exhibit hypocalcemia, hypophosphatemia, secondary hyperparathyroidism, elevated alkaline phosphatase, normal 25-(OH)D levels and extremely high levels of 1,25-$(OH)_2$D which can be the first biochemical evidence of HVDRR (**Table 2**) (Tiosano et al., 2001; Malloy et al., 2011). Due to the wide spectrum of VDR mutations in this disease, treatment of these patients can vary. Patients who retain partial activity of VDR can be treated with high doses of 25-(OH)D or 1,25-$(OH)_2$D (Malloy et al., 1999), while patients who have end organ resistance to calcitriol and complete loss of activity of VDR require long term intravenous calcium supplementation (Weisman et al., 1987). However, these patients can be shifted to high-dose oral calcium therapy after radiological healing of their rickets (Hochberg et al., 1992). The phenomenon of alopecia in these patients is quite interesting and is attributed to mutations in *VDR* disrupting important ligand-independent actions of the vitamin D receptor that are required for hair follicle development (Skorija et al., 2005). It is now generally agreed upon that patients presenting with alopecia are more resistant to treatment than others (Malloy et al., 2011). As in the case of PDDR, a mouse model was engineered to mimic the HVDRR phenotype (Li et al., 1997; Yoshizawa et al., 1997); these mice first appeared normal at birth but progressively became rachitic, alopecic, and developed hypocalcemia with secondary hyperparathyroidism. Excluding alopecia, these abnormalities were successfully corrected with a calcium rescue diet (Li et al., 1997; Yoshizawa et al., 1997; Malloy et al., 2010).

Table 2: Comparison between 1α-Hydroxylase deficiency (PDDR) and HVDRR. Taken from (Malloy et al., 2011).

Feature	**1α-Hydroxylase deficiency**	**HVVDRR**
Gene mutated	CYP27B1	VDR
Autosomal recessive	Yes	Yes
Manifested at early age	Yes	Yes
Rickets	Yes	Yes
Hypocalcemia	Yes	Yes
Alopecia	No	Sometimes
PTH	Elevated	Elevated
25-(OH)D levels	Normal	Normal
1,25-$(OH)_2$D levels	Normal	Elevated
Response to physiological doses of 1,25-$(OH)_2$D	Yes	No

The identification of the underlying genetic mutations of these disorders, as well as the successful engineering of their respective mouse models highlight the critical roles 1,25-$(OH)_2$D and VDR have in skeletal maturity, bone health and mineral ion homeostasis. The prevalent view is that correction of mineral ion homeostasis by normalizing serum calcium and phosphorus levels is sufficient to correct skeletal abnormalities, but despite that, it only maintains a transient developmental role and thus cannot fully substitute for vitamin D action. This proves that the calcium ion system and the 1,25-$(OH)_2$D/VDR system each exert different effects on the skeletal system that either occur coordinately or independently (Panda et al., 2004).

1.3 CYP24A1 and 24,25-$(OH)_2D$

We have described how the activation process of vitamin D involves a cascade of hydroxylation steps involving many enzymes in different sites of the body; unsurprisingly, the inactivation of 1,25-$(OH)_2D$ and its catabolic breakdown also involve a series of successive hydroxylations. The critical enzyme involved in the degradation of calcitriol is CYP24A1. In fact, and in a classic negative feedback loop, 1,25-$(OH)_2D$ seems to play a key role in regulating vitamin D homeostasis by activating transcription of *CYP24A1* subsequently resulting in its own catabolic breakdown (St-Arnaud, 2011).

CYP24A1 is a mitochondrial inner-membrane enzyme that belongs to the family of cytochrome P450 enzymes (St-Arnaud, 2011). It is expressed in almost all 1,25-$(OH)_2D$ target tissues, but similarly to CYP27B1 it has a preferential concentration in the kidney (Ohyama et al., 1991; Omdahl et al., 2002). This enzyme has the ability to hydroxylate both 25-(OH)D and 1,25-$(OH)_2D$ at either carbon number 23 (C23- hydroxylation) or number 24 (C24- hydroxylation) (Petkovich et al., 2011), and although its affinity for 25-(OH)D is lower than that for 1,25-$(OH)_2D$ (Burgos-Trinidad et al., 1991; Inaba et al., 1991; Sakaki et al., 2000), in vitro studies have shown that both are catabolized at a similar rate (Masuda et al., 2004). Before describing the C23- and the C24- hydroxylation pathways in detail, it is worth mentioning that the utilization of these pathways by CYP24A1 can be species dependent. Humans are able to use both pathways equally (Beckman et al., 1996; Sakaki et al., 2000) while the guinea pig preferentially uses the C23- pathway (Pedersen et al., 1988), contrary to rats (Sakaki et al., 1999) and mice (Engstrom et al., 1986) who preferentially use the C24- pathway. The pathways will be described below.

1.3.1 Hydroxylation Pathways

1.3.1.1 C23-Hydroxylation

In general the carbon 23 hydroxylation pathway of 1,25-$(OH)_2$D and 25-$(OH)_2$D contains fewer steps than the 24 hydroxylation pathway of these metabolites. 1,25-$(OH)_2$D is transformed first into 1,23S,25-$(OH)_3$D and then into 1,23S,25,26-$(OH)_4$D by successive hydroxylation at carbon 23 and carbon 26. The latter molecule is transformed into 1,25-$(OH)_2$D-26,23-lactol from where it becomes the final product of 1,25-$(OH)_2$D-26,23-lactone that is excreted by the kidney (**Figure 6**) (St-Arnaud, 2011). The same steps apply to 25-(OH)D which is first transformed into 23,25-$(OH)_2$D, then 23,25,26-$(OH)_3$ that is converted into 25-(OH)D-26,23-lactol and finally 25-(OH)D-26,23-lactone (Ishizuka et al., 1987). The biological activity of the C23- pathway metabolites remains a bit unclear (St-Arnaud, 2011), but it has been postulated that the lactone end product could serve as a VDR antagonist (Toell et al., 2001; Ishizuka et al., 2005) to further augment vitamin D signaling inhibition (St-Arnaud, 2011).

1.3.1.2 C24-Hydroxylation

This pathway involves five separate enzymatic steps that eventually result in the degradation metabolite calcitroic acid. 1,25-$(OH)_2$D is first hydroxylated at carbon number 24 resulting in 1,24,25-$(OH)_3$D that is then ketonized to 24-oxo-1,25-$(OH)_2$D. The following step is the hydroxylation of carbon 23 generating 24-oxo-1,23,25-$(OH)_3$D. Oxidative cleavage of the bond between C23 and C24 produces 24,25,26,27-tetranor-1,23-$(OH)_2$D which is then converted to calcitroic acid that is excreted in the bile (**Figure 6**) (Beckman et al., 1996; Sakaki et al., 1999; St-Arnaud, 2011). 25-(OH)D metabolism through this pathway also results in calcitroic acid excreted in the bile and the intermediate metabolites of its degradation are 24,25-$(OH)_2$D, 24-oxo-25-(OH)D, 24-oxo-23,25-$(OH)_2$D and 24,25,26,27-tetranor-23-(OH)D (St-Arnaud, 2011).

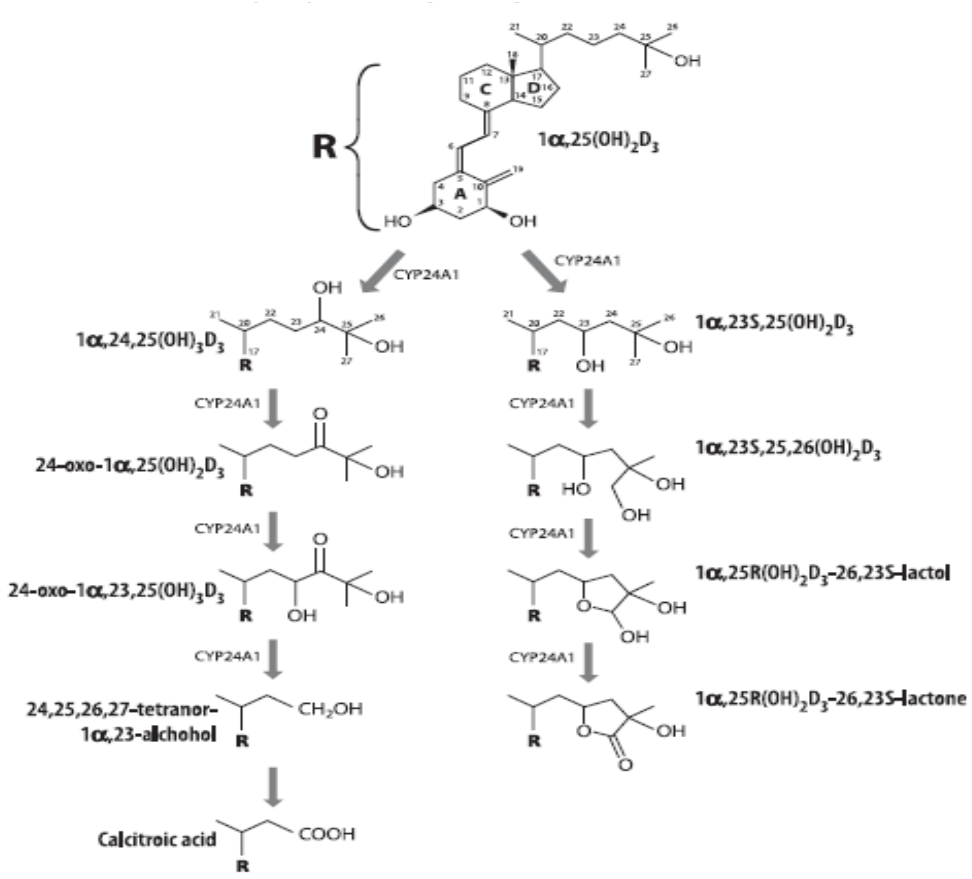

Figure 6: 1,25-$(OH)_2D$ degradation pathway by CYP24A1. Left: C-24 oxidation pathway. Right: C-23 oxidation pathway. Refer to text for 25-(OH)D products. Taken from (St-Arnaud, 2011).

1.3.2 Identifying a Role for CYP24A1 in Mineral Ion Homeostasis

From what we have so far mentioned, it would seem that the sole purpose of CYP24A1 is to enforce tight vitamin D control by catabolically breaking down 1,25-$(OH)_2D$ and 25-(OH)D, rendering the intermediate metabolites (such as 24,25-$(OH)_2D$) mere degradation metabolites with no physiological function. Many studies validate this idea by showing that this enzyme and its degradation metabolite 24,25-$(OH)_2D$ show no significant effects on classical actions of vitamin D. When vitamin D analogs were fluorinated at carbon number 24 (making this carbon inaccessible to CYP24A1 and hydroxylation) and were given

to vitamin D-deficient rats, no significant differences were seen between that group and to the group given 25-(OH)D with respect to bone mineralization, calcium mobilization from bone, healing of rachitic epiphyseal plate cartilage or on intestinal calcium transport (Tanaka et al., 1979). Other studies further validated this notion by demonstrating that the embryonic development of chicken (Ameenuddin et al., 1982) and normal growth and reproduction in rats (Jarnagin et al., 1983) was dependent on 1,25-$(OH)_2$D and not 24,25-$(OH)_2$D. These findings do not by any mean undermine the relevance of the crucial role CYP24A1 plays in the catabolic breakdown of 1,25-$(OH)_2$D and 25-(OH)D as part of the tight regulation of vitamin D levels. It has been shown recently that inactivating mutations in *CYP24A1* result in a syndrome called "Idiopathic Infantile Hypercalcemia". Patients with this syndrome present early on in life (especially after supplementation with vitamin D) with weight loss, failure to thrive, dehydration and hypotonia. Laboratory analysis of these patients shows profound hypercalcemia, low levels of PTH and hypercalciuria (Schlingmann et al., 2011). This clinical spectrum highlights the importance of CYP24A1 in mineral ion homeostasis but does not describe an additional physiological role for this enzyme.

With time, researchers began looking for a potential role for CYP24A1 and 24,25-$(OH)_2$D using an approach that did not solely focus on possible effects of this enzyme in the classical function of vitamin D. Since chondrocytes express enzymes that allow for the synthesis of both 1,25-$(OH)_2$D and 24,25-$(OH)_2$D, it has been postulated that the latter might play a role in chondrocyte differentiation and function. In fact, resting cartilage cells respond primarily to 24,25-$(OH)_2$D and the activity of alkaline phosphatase, phospholipase A_2 and protein kinase C seem to be regulated by this metabolite (Schwartz et al., 1988; Schwartz et al., 1988). In vitamin D-deprived growing chicken, 24,25-$(OH)_2$D was shown to have healing effects on rachitic lesions; supplementation of these chicken with 1,25-$(OH)_2$D was able to normalize calcium and phosphorus levels but had no effect on reversing the lesions proving that the former metabolite might play a critical role in bone formation (Ornoy et al., 1978). In support of these

observations, other studies were able to show that both 1,25-$(OH)_2$D and 24,25-$(OH)_2$D were vitally important for normal egg hatchability and not just 1,25-$(OH)_2$D alone (Henry et al., 1978; Norman et al., 1983).

The search for a physiological role of CYP24A1 and 24,25-$(OH)_2$D continued and it was shown that this metabolite had some interesting effects on bone mass and mechanical strength. With the administration of 24,25-$(OH)_2$D to vitamin D-replete rabbits, bone mineral content and strength increased in these mammals in comparison to their control groups despite lack of change in 25-(OH)D and 1,25-$(OH)_2$D levels (Nakamura et al., 1992; Nakamura et al., 1992). To further support these observations, ovariectomized dogs treated with 24,25-$(OH)_2$D showed increased bone mass and decreased bone resorption than the non-treated control dogs (Nakamura et al., 1992). These studies and beneficial effects of 24,25-$(OH)_2$D do not clearly establish a putative physiological role for the metabolite, but show clearly that it exhibits pharmacological effects that play a critical and essential role in bone health, strength and maturity.

1.3.3 The Effects of CYP24A1 and 24,25-$(OH)_2$D on Fracture Repair

The search for a potential role for 24,25-$(OH)_2$D in bone health took a further step in trying to identify a role for it in fracture repair. After inducing tibial fractures in chicken, a gradual increase in kidney CYP24A1 activity was seen with a peak at day 10 followed by a gradual decrease to baseline around day 15 post-fracture. These observations were accompanied by an increase in serum levels of 24,25-$(OH)_2$D that followed the same pattern (Seo et al., 1997). The same group then studied the role of 24,25-$(OH)_2$D on bone repair and noticed that when this metabolite was added to the chicken diet, it was sufficient by itself to achieve optimal bone repair and integrity compared to controls fed 1,25-$(OH)_2$D alone. In addition the biomechanical parameters such as torsional strength, stiffness and angular deformation of the fracture calluses were superior in chicks fed 24,25-$(OH)_2$D than those fed 1,25-$(OH)_2$D alone (Seo et al., 1997).

To further study the effects of 24,25-$(OH)_2D$ on fracture repair in close relation to human biology, it was imperative to develop a mouse model that would allow such studies to be performed. The *Cyp24a1*$^{-/-}$ mouse (St-Arnaud et al., 2000) serves as an invaluable tool to examine the role of 24,25-$(OH)_2D$ in mammalian fracture repair.

1.4 Engineering the Cyp24a1 Gene Deficient Mouse

Our laboratory was successful in engineering a mouse deficient for the *Cyp24a1* gene in order to study the effect of this mutation on vitamin D homeostasis and bone formation. This was done by the removal of the heme-binding domain sequences at exons 9 and 10 of the gene generating a null allele (**Figure 7**) (St-Arnaud et al., 2000). *Cyp24a1* mRNA levels could not be detected in the mutant mice, and compared to their wild-type (WT) counterparts, these mice exhibited decreased blood circulating levels of 24,25-$(OH)_2D$. To check and confirm lack of CYP24A1 enzyme activity in the mutant mice, an acute bolus of 1,25-$(OH)_2D$ was injected in these mice and their wild-type counterparts. Unlike the mutant mice, the wild-type mice were successful in clearing the bolus and re-normalizing their 1,25-$(OH)_2D$ blood levels (**Figure 8**); these findings were reproduced with chronic 1,25-$(OH)_2D$ injections (St-Arnaud et al., 2000). Interestingly, 50% of the mice homozygous for the mutation died before 3 weeks of age (**Table 3**) (St-Arnaud, 1999). After eliminating potential reasons as to be the cause of this phenomenon, it was determined that the cause of perinatal lethality is hypercalcemia caused by excess levels of circulating 1,25-$(OH)_2D$ (St-Arnaud et al., 2000). The fact that 50% of the homozygous mutant animals survived to adulthood when vitamin D homeostasis and calcemia is not challenged allowed successful breeding and the examination of the effect of the complete lack of CYP24A1 activity on bone development; in fact, homozygous mutants born of homozygous females exhibit abnormal bone development with excess accumulation of osteoid at sites of intramembranous ossification with severely reduced amounts of bone in the mandibles of these mice (St-Arnaud et al., 2000).

Supplementation of mutant females with 24,25-$(OH)_2D$ during gestation did not rescue the phenotype, however double mutant homozygotes of *Cyp24a1* and *Vdr* show normal intramembranous formation at all sites (St-Arnaud et al., 2000). These results establish the CYP24A1 enzyme as a key regulator of 1,25-$(OH)_2D$ homeostasis, and that the phenotype exhibited by the *Cyp24a1* deficient mice was in fact due to the exaggerated and unopposed effects of high circulating levels of 1,25-$(OH)_2D$. The successful breeding of these mutant mice in considerable numbers allowed us to perform all our surgical experiments.

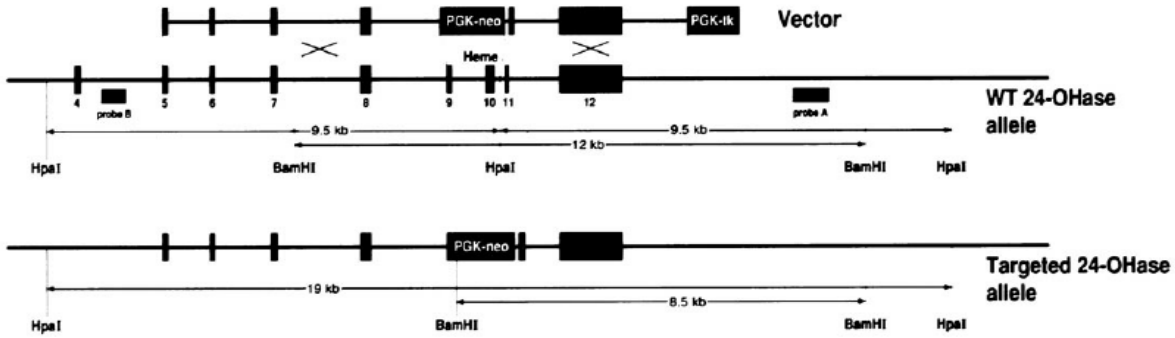

Figure 7: Inactivation of the *Cyp24a1* gene in mice by removal of the heme-binding domain sequences at exons 9 and 10**.** Taken from (St-Arnaud et al., 2000).

Table 3: Fifty percent of the mice homozygous for the mutant *Cyp24a1* gene die at weaning. Taken from (St-Arnaud, 1999).

Number of -/- embryos	Alive at weaning	Dead at weaning
35	18 (51%)	17 (49%)

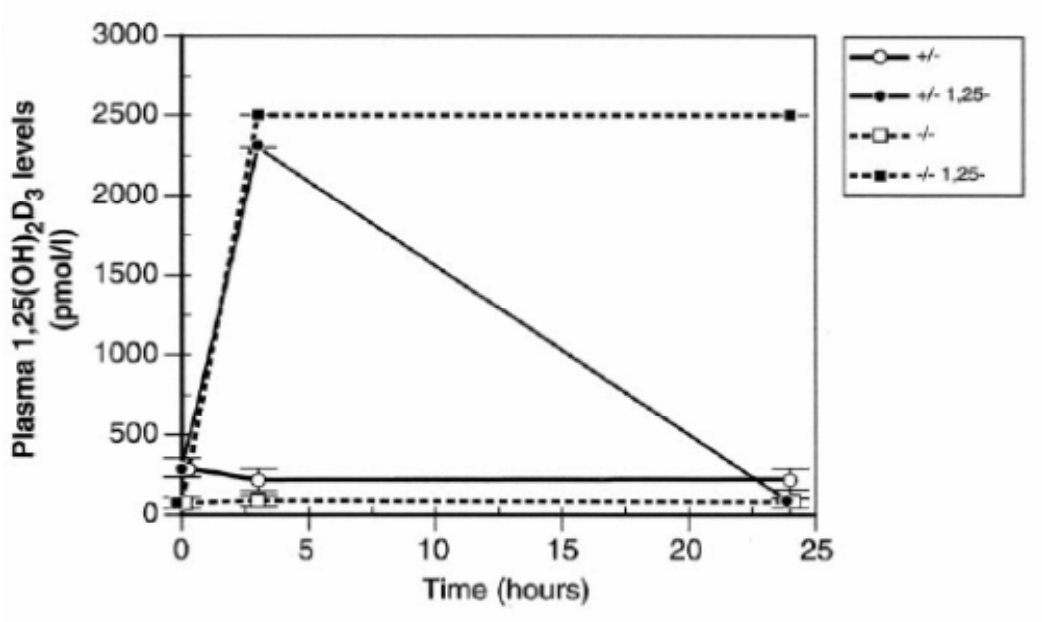

Figure 8: Impaired vitamin D catabolism in *Cyp24a1*$^{-/-}$ after acute bolus injection of 1,25-$(OH)_2$D; normal catabolism in heterozygote littermates. Taken from (St-Arnaud et al., 2000).

Our previous studies comparing fracture repair between these mutant mice and their wild-type littermates have shown delays in mineralization of the cartilaginous matrix of the soft callus that is accompanied biochemically by reduced gene expression of chondrocyte markers; this highly suggests that this metabolite plays a critical role in mammalian fracture repair (St-Arnaud, 2010). To further augment the hypothesis that 24,25-$(OH)_2$D is a key factor in optimizing fracture repair, our laboratory has previously compared callus formation between wild-type and mutant mice, in the presence or absence of exogenous 24,25-$(OH)_2$D at different time points post-osteotomy using two different surgical modalities (Naja, 2008; Husseini, 2011). Histological analysis of fracture calluses from both types of mice at day 14 showed significantly poor development in the mutant mice compared to the wild-type mice. Upon exogenous administration of 24,25-$(OH)_2$D, histology of the fracture calluses at day 14 in the mutant mice showed normal development as seen in the wild-type mice, whereas administration of 1,25-$(OH)_2$D was not able to rescue the calluses. These results suggest that this metabolite plays a critical role in optimizing fracture healing (Naja, 2008). In support of these observations, micro-CT analysis

and bone histomorphometry studies both showed that there was a consistently lower bone volume per tissue volume (BV/TV) in the mutant mice compared to the wild-type mice at days 10, 14 and 18 post-osteotomy, but not at day 28 post-osteotomy (**Figure 9A**). These differences disappeared in the mutant mice after exogenous administration of 24,25-$(OH)_2D$ (**Figure 9B**) (Husseini, 2011). These results clearly show that 24,25-$(OH)_2D$ plays a critical role in optimizing fracture repair.

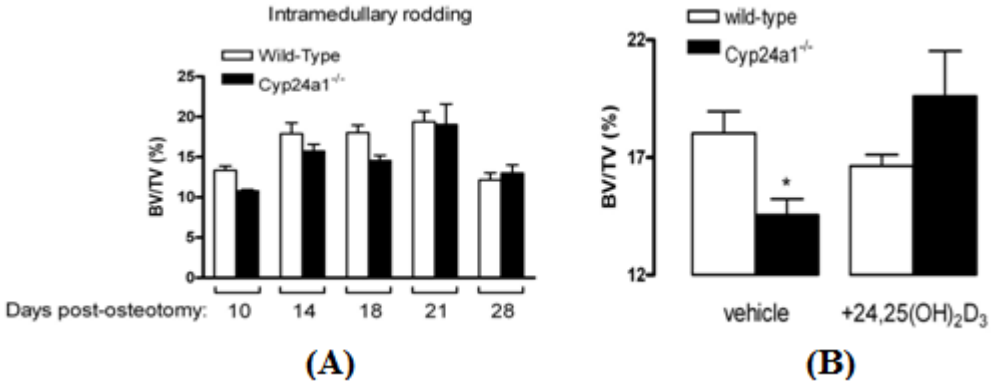

Figure 9: Consistently lower BV/TV in mutant mice compared to wild-type mice at 10, 14 and 18 days post-osteotomy. No differences seen at days 21 and 28 post-osteotomy **(A)**. Dissappearance of differences in BV/TV between wild-type mice and mutant mice after exogenous administration of 24,25-$(OH)_2D$ **(B)**. Taken from (Husseini, 2011).

1.5 Identifying a Receptor for 24,25-$(OH)_2D$

Previous studies mentioned above have established the fact that 24,25-$(OH)_2D$ plays a major role in fracture repair and bone health, but none of these studies identified the exact molecular mechanism underlying the effects of this metabolite. Other groups have tried to characterize and identify a receptor specific for 24,25-$(OH)_2D$ that will explain the molecular basis of the effects seen in the animal models studied. Studies in chicken and dogs suggested that the parathyroid gland might be a potential location for the activity of 24,25-$(OH)_2D$ (Canterbury et al., 1978; Chertow et al., 1980), while more recent studies have focused on fracture calluses as the site of the metabolite's action, where a membrane binding protein was shown to have high affinity for 24,25-$(OH)_2D$ but not to 1,25-$(OH)_2D$

(Seo et al., 1996). The success of our laboratory in engineering a mouse deficient for *Cyp24a1* (St-Arnaud et al., 2000) allowed us to perform a search for a putative specific receptor of 24,25-$(OH)_2D$ in a mammalian model. It was reasoned that 24,25-$(OH)_2D$ would act through receptor-mediated signaling in fracture repair, therefore it was hypothesized that the metabolite's receptor would be up-regulated in the *Cyp24a1*$^{-/-}$ fracture calluses. Gene expression monitoring by cDNA microarrays of fracture calluses at day 14 post-operation from wild-type or *Cyp24a1*$^{-/-}$ showed the over-expression of 4 genes with no described function, of which one (1500016O10Rik), known as *Family with sequence similarity 57 member B* (*Fam57b*) was predicted to encode a transmembrane protein. Further experiments done by our laboratory were able to show that *Fam57b* binds 24,25-$(OH)_2D$ in a specific and saturable manner when the gene was expressed in the fibroblast like COS-7 cells (**Figure 10**). No specific binding was measured when the cells were transfected with empty vectors or with expression vectors for the other overexpressed clones. These results suggest that *Fam57b* is a gene that encodes a transmembrane receptor for 24,25-$(OH)_2D$.

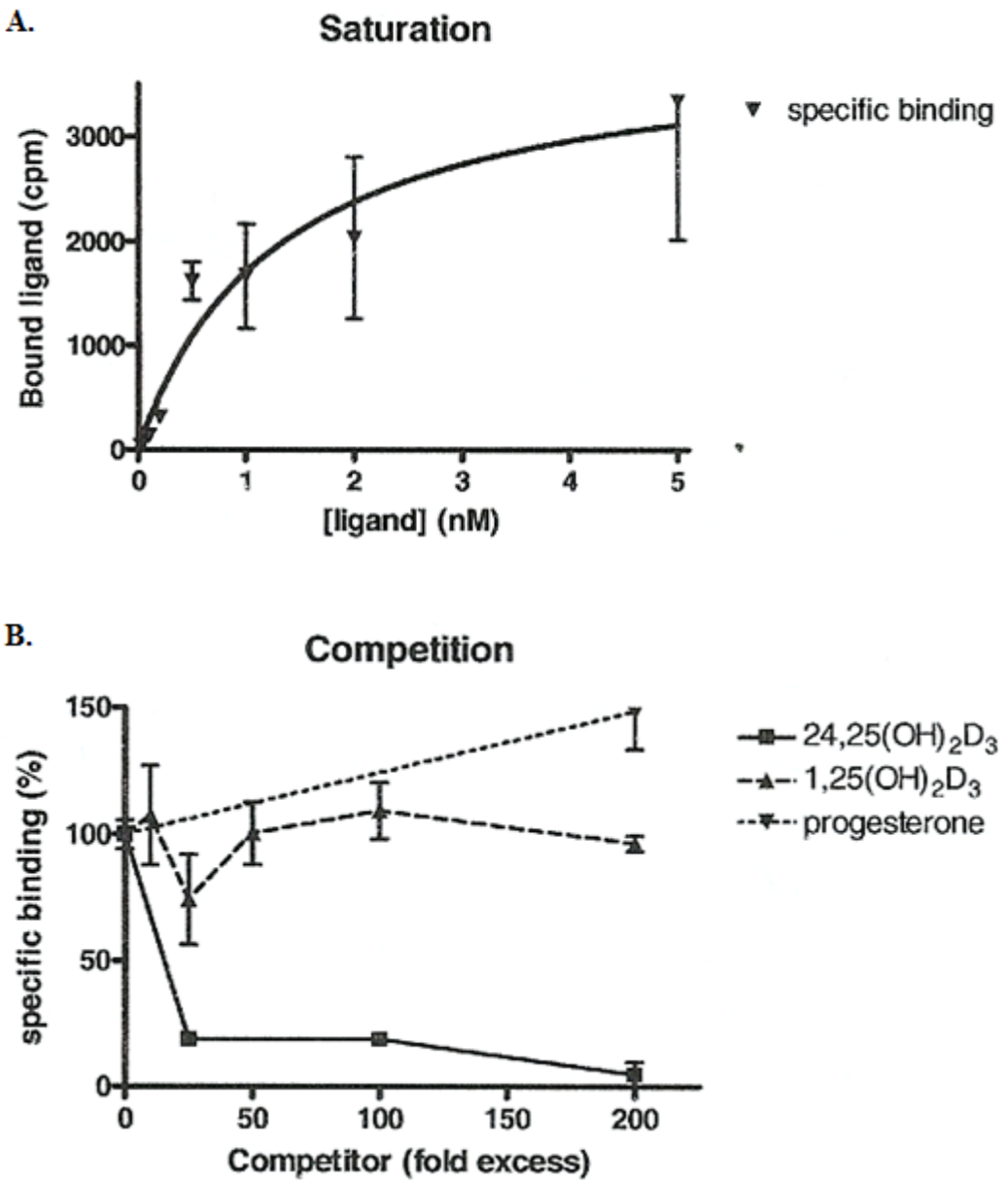

Figure 10: **A.** Saturable and specific binding of radioactive [^{3}H]-24,25-$(OH)_2$D to FAM57B. **B.** Binding was displaced by cold 24,25-$(OH)_2$D but not by 1,25-$(OH)_2$D or progesterone. Reference not published.

1.6 Fracture Repair

Fractures are one of the most frequent injuries of the musculoskeletal system (Claes et al., 2012). A fracture is basically a crack or a break that disrupts the normal architecture of the bone (Frost, 1989). The majority of tissues in the body heal by the formation of a poorly organized scar after being subjected to an insult, on the other hand, fracture healing results in the regeneration of the original tissue (bone) while largely restoring the properties of that tissue prior to injury (McKibbin, 1978; Einhorn, 1998). This process is achieved by an orchestra of biological events involving cellular responses, signaling pathways, adequate vascularization and proper mechanical stabilization. It is agreed upon nowadays that fracture healing occurs through three overlapping phases that are the initial inflammatory phase, the reparative phase and finally the remodeling phase. The reparative phase constitutes two different types of bone healing depending on the type of fracture. Direct or primary bone healing occurs without a cartilaginous intermediate (callus), while indirect or secondary bone healing occurs with the formation of a precursory callus stage (Frost, 1989; Einhorn, 1998; Claes et al., 2012). Most sustained fractures are treated with forms of surgical management that allow minimal motion between the two ends of bone such as cast or sling immobilization, external fixation or intramedullary (IM) fixation, and accordingly most of the fractures heal through secondary healing, rendering primary bone healing a rarity (Einhorn, 1998). For the sake of this work, we will discuss secondary bone healing only.

1.6.1 Phases of Fracture Repair

1.6.1.1 Inflammatory Phase

This is the first phase after initial bone insult and typically lasts over a course of seven days. It serves as a starting point and attracts all the required molecules to initiate the cascade of events that are required for full healing and repair of the

bone (Frost, 1989). When a fracture occurs, it results in blood vessel rupture inside the bone and the surrounding tissue, promoting the start of the inflammatory cascade with vasodilation and exudation of plasma (Wray, 1964; McKibbin, 1978; Kolar et al., 2010). These events along with the death of the bone ends allows the creation of a hematoma (Aho, 1966) within the fracture gap characterized by hypoxia, low pH, and an abundance of inflammatory cells and cytokines (Kolar et al., 2010); it acts as a scaffold for the invasion of additional inflammatory cells (polymorphonuclear cells, macrophages and lymphocytes) (Claes et al., 2012). As a result of the hypoxia, many angiogenic factors are released at the fracture site (Ai-Aql et al., 2008) promoting revascularization which is essential for removing debris and providing a source of access to osteoprogenitor cells (Claes et al., 2012). Fibroblasts are then mobilized to the fracture site and the hematoma begins to be replaced by granulation tissue composed of collagen fibers (McKibbin, 1978) commencing the repair phase.

1.6.1.2 Repair Phase (Secondary Healing)

The reparative phase overlaps with the inflammatory phase and continues for several weeks (Einhorn, 1998). Fractures treated by external fixation or IM nails are allowed a considerable degree of movement between the fragments and thus secondary bone healing is the predominant form of healing in these fractures. Two processes are involved in this type of repair: intramembranous and endochondral bone formation (McKibbin, 1978; Frost, 1989; Claes et al., 2012).

Intramembranous bone formation begins to occur for around two weeks after the fracture and is characterized by direct differentiation of periosteal precursor cells into osteoblasts, without the formation of a cartilaginous intermediate. This is believed to occur in places where the periosteum and vascularization were not completely damaged by the fracture and where there is minimal interfragmental movement (McKibbin, 1978; Claes et al., 2012). These osteoblasts lay down woven bone around the fracture site and this area is often referred to as the “hard callus” (Einhorn, 1998). In other areas of the fracture, endochondral ossification is

the predominant type of repair. This process is driven by chondrocytes and results in the formation of a cartilaginous tissue, the "soft callus" (McKibbin, 1978; Claes et al., 2012). This process is possible due to the fact that chondrocytes, unlike osteoblasts, have the ability to differentiate and proliferate in areas of low oxygen and decreased blood supply (McKibbin, 1978). When these chondrocytes eventually hypertrophy and undergo apoptosis, they release calcium which then causes a decrease in interfragmentary movement. This allows blood vessels to invade this calcified cartilage, delivering monocytes and mesynchymal stem cells to the site that develop into osteoclast-like cells and osteoblasts respectively. This process can range from four to sixteen weeks until the whole fracture site is turned into a network of dense woven bone and paves the way for the remodeling phase (Einhorn, 1998).

1.6.1.3 Remodeling Phase

This is the last and final stage of fracture healing that can take up to many years in humans (Frost, 1989; Claes et al., 2012). In this stage the levels of inflammatory cytokines begin to drop and vascularization is reduced to pre-fracture levels. The hall mark of this stage is the resorption of the excess callus and woven bone by the osteoclasts and the deposition of more compact lamellar bone (similar to primary bone healing), that is aligned along the loading axis of the original bone (Buckwalter, 1996). The final outcome is a fully-loadable reconstructed bone (Claes et al., 2012).

1.7 Intamedullary Nails

Intramedullary nails are long metallic rods that can be used in surgical repair of long bone fractures. They are inserted into the medullary canal of the long bone with the purpose of stabilizing and supporting the fracture. The evolutionary process of IM nails has been huge and many advances have been made that

allowed surgeons to effectively treat a multitude of fracture types (Mazzocca et al., 2003).

There are two types of IM nails: Non-locking and locking. Non-locking nails are nails that are not stabilized with screw or pin fixation. This type of fixation allows a degree of movement of the fragments allowing axial and rotational movements while supporting bending. These types of nails are indicated when the reduced fracture has adequate rotational stability and thus will resist twisting when loaded. Since these types of nails allow a certain degree of inter-fragmentary movement, secondary bone healing through endochondral ossification and the formation of a precursory callus is observed. Locking nails on the other hand have a series of regularly spaced holes that pass through the axilla of the nail on all four sides, thus allowing screws to be inserted from any direction resulting in rigid fixation of the nail (**Figure 11**). These are the preferred nails to stabilize rotationally unstable and comminuted fractures of the long bones of the leg. Due to the high stability of these nails, the predominant type of bone healing is primary without the formation of a cartilaginous callus (Mazzocca et al., 2003).

We have used non-locking nails in our experiments (detailed below) and thus have studied endochondral bone formation during fracture repair.

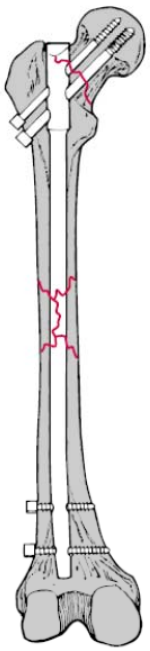

Figure 11: Schematic representation of a locking nail used to treat a femoral neck and comminuted shaft fracture. Taken from (Mazzocca et al., 2003).

1.8 Bone Biomechanics

The bones of the skeleton serve many roles in the human body of which at least two are key biomechanical roles. The first role is the protection and shielding of vital organs from trauma where many of the bones are structured in a sandwich-like form of which a compliant core (spongy bone) separates two stiff plates. For example, when the skull is subjected to blunt trauma, mechanical energy concentrates mainly in the core and thus little of that energy is transferred to the innermost bony plate consequently protecting the brain from damage. The second role of bones is to function as levers against which muscles contract. Bones are generally shaped in a way that optimally distributes joint forces; the ends of the long bones are usually broad which reduces stress (force per unit area), and the stress is transmitted by the trabecular bone in the metaphysis into the long bone cortex (Burr, 2003). In this section we define the basic terminology and fundamental principles of bone biomechanics, along with the different modalities available for biomechanical testing that serve as the core of this work.

1.8.1 Stress-Strain Curve

Defining the components of the stress-strain curve is fundamental to understand bone biomechanics. Stress is defined as the force per unit area and can be classified as compressive (material becomes shorter), tensile (material is stretched), or shear stress (one region slides relative to an adjacent region) (Turner et al., 1993). Strain is the percentage change in length, or the relative deformation of the material. The relationship between stress and strain in bone follows the shape of a curve which is called the stress-strain curve; the components of this curve allow the biomechanical comparison of different samples (**Figure 12**) (Turner et al., 1993).

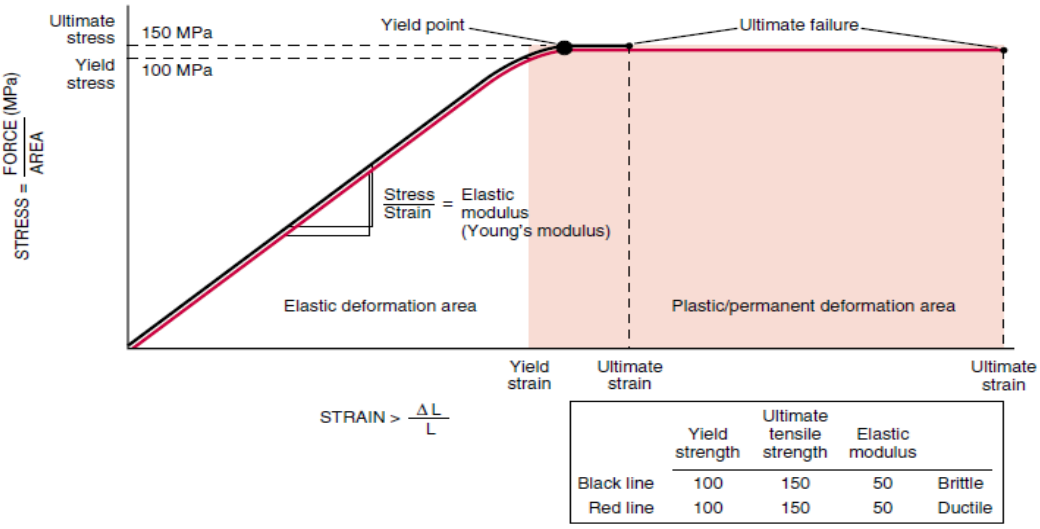

Figure 12: Stress-Strain curve. Detailed explanation below. Taken from (Mazzocca et al., 2003).

The *yield point* is the force required to induce the earliest permanent change in shape or deformation of the sample; it divides the curve into two parts, the elastic deformation area and the plastic/permanent deformation area. *Elasticity* is the ability of the sample to restore its original shape after the deforming force is removed. It is quantified by the slope of the curve in the elastic region which is called *young's modulus*; this parameter defines the *stiffness* of the bone

(Mazzocca et al., 2003). Stresses beyond the *yield point* will cause permanent damage to the bone structure which is called *plastic deformation*. Ductile materials have the ability to deform beyond the *yield* point before fracture whereas brittle materials lack that ability (Mazzocca et al., 2003). In general bone is a not a very ductile material and thus has little ability to sustain post-yield deformation. Therefore the less brittle the bone is, the more it can withstand stress after the *yield point* before fracture (Turner et al., 1993). The force that is required to break the bone corresponds to the *ultimate stress*. Finally the total amount of energy required to break the bone is the *toughness* and it is defined by the area under both parts (plastic and elastic) of the curve (Mazzocca et al., 2003).

1.8.2 Biomechanical Testing of Healing Bone

Many modalities can be used to assess the biomechanical properties of healing bone or fracture calluses in laboratory settings such as torsion, three-point bending, tension, and compression. Loading the bone in tension is when the two halves are pulled apart, while loading it in compression is when the fractured ends are compacted against one another. These two modalities are not commonly used in laboratory settings when assessing long bones. Since long bones in vivo experience bending and torsional moments, torsion and three-point bending are most commonly used to assess fracture healing in the laboratory. Testing the bone in torsion is twisting the two halves of the bone until failure, while in three-point bending the bone is placed horizontally on two vertical supports and a third rod bends the bone from the top until it breaks. The disadvantage of three-point bending is that it creates a non-uniform bending moment throughout the fracture callus and thus failure does not necessarily occur at the weakest cross-section. On the other hand torsion testing subjects every point of the callus to the same torque, but due to its simplicity and practicality, three point bending is the preferred method. Irrespective of the modality used, all biomechanical outcome measures mentioned above can be derived and obtained such as *stiffness, toughness* and *ultimate stress* (force to break) (Morgan et al., 2009).

1.8.3 Biomechanical Stages of Fracture Healing

There are four biomechanical stages of fracture healing that were defined using the results of torsional testing performed on healing rabbit tibias at multiple time points (White et al., 1977). It should be noted that the duration of each stage is species dependent, i.e. healing in smaller animals (mice) progresses more rapidly than in larger animals (rabbits). Stage 1 is characterized by extremely low stiffness and strength of the callus and occurs at the original fracture line. This stage corresponds to the inflammatory phase of fracture healing. Stage 2 corresponds to increased callus stiffness and corresponds to the soft callus phase and the beginning of the bony callus phase in the repair phase of fracture healing. Stage 3 is characterized by further increase in stiffness and is where failure occurs partly outside the original fracture line. In stage 4, failure in the torsion test occurs in intact bone rather than the original fracture line. The transition from stage 3 to 4 corresponds to the beginning of the remodeling phase of fracture healing (Morgan et al., 2009).

2. Aims of the Study

2.1 mRNA and Protein Expression

To assess the RNA and protein expression of a presumed specific receptor for 24,25-$(OH)_2D$ in different mice organ tissues.

2.2 Biomechanical Testing

To use a previously devised small animal surgical model of a tibial fracture to assess the biomechanical properties of fracture calluses in *Cyp24a1* gene deficient mice.

3. Original Contributions to the Aims

This work describes a number of results and techniques that were achieved and developed in our laboratory by my present and former colleagues. Those results and techniques played a crucial and key role in achieving the aims of this work, and thus this section distinguishes my specific original contributions from those of my colleagues'. Regarding the first aim, the plots shown in **Figure 10** were performed by a colleague of ours in the laboratory, Claude Gauthier, but were never published. However, they served as a starting point to achieve the first aim of this work that is described in **Figures 16-20** that reflect my original contributions. With respect to the second aim, the surgical modality used in this work was developed by Abdallah Husseini, a former masters student in our labortatory, and is depicted in **Figures 13** and **14**. The results of Dr. Husseini's work are shown in **Figure 9**, and serve as a base to my original results in this work that are shown in **Figures 21-24**. **Figure 15** was taken from the web and all other figures are adapted from the literature, with appropriate referencing.

4. Materials and Methods

4.1 mRNA Quantification

4.1.1 RNA Extraction from Tissues

Twelve week old wild-type mice were euthanized using CO_2 asphyxia. The mice were dissected and the following organs were collected in 17x100 mm culture tubes containing 2-3 ml RNA Later solution (Ambion Inc., # AM7021, Austin, USA): Kidney, heart, brain, skin (without hair), muscle, tibia without the epiphysis (flushed bone marrow with normal saline), calvaria, small intestine, and rib cartilage. The RNA Later was poured out and the samples were cut into small pieces, with the exception of the bone sample that was frozen with liquid nitrogen and crushed using a pestle and mortar. The samples were transferred to 17x100 mm culture tubes containing 2 ml of Trizol reagent (Invitrogen Inc., Carlsbad, USA) and then homogenized by a Polytron (PT-MR 3000 Kinematica, Switzerland). They were then centrifuged at 4°C for 10 mins, and the supernatant of each sample was divided into 1 ml eppendorf tubes. To each tube, 200 µl of chloroform were added and the tubes were shaken vigorously and then centrifuged for 15 mins at 4 degrees at 12000 RCF. The colorless aqueous supernatant was transferred to fresh new 1 ml eppendorf tubes and 500 µl of isopropanol were added to each tube. The tubes were shaken vigorously and left to stand for 10 mins at room temp. They were then centrifuged for 10 mins at 4°C at a speed of 12000 RCF. The supernatant was then poured out with caution as to not disturb the pellet and 1 ml of ethanol (75%) was then added to the tubes. The tubes were then centrifuged for 5 mins at 4°C at a speed of 7600 RCF. The ethanol was removed from the tubes using a 200 µl pipette and they were left to air dry for 30 mins. Finally, 30 µl of RNAase free water were added to the tubes and reverse transcription was started.

4.1.2 Reverse Transcription

Reverse transcription of the isolated mRNA was done by using the High-Capacity cDNA reverse transcription kit (Applied Biosystems #4368813, Branchburg, USA) following the manufacturer's instructions. The kit successfully reverse-transcribes tissue RNA into cDNA by the use of random primers and multiscribe reverse transcriptase. The volume of mRNA to be reverse-transcribed (corresponds to 1 µg) was added to 20 µl of RNAse-free water. The master mix was prepared according to the instructions supplied with the kit, and 20 µl were added to each tube containing the mix of mRNA and RNAse-free water. The samples were then revere-transcribed to cDNA using the GeneAmp PCR 9700 thermal cycler (Applied Biosystems, Branchburg, USA).

4.1.3 Quantitative Real-time reverse transcription PCR (qRT-PCR)

The relative expression of *FAM57B* (Mm01276190) and *Fam57Bv2* (Mm01276192_m1) from the cDNA obtained from the above mentioned samples was measured using qRT-PCR. The machine that was used for this process was the Applied Biosystems 7500 instrument (Applied Biosystems, Branchburg, USA). In this machine, quenched fluorescent probes interact with the cDNA templates, and upon amplification, the degradation of the probes releases fluorescence. This provides the Ct value, which is a quantitative assessment of the mRNA of the gene of interest. This Ct value is normalized to the Ct value of the housekeeping control gene that we used which is *Gapdh* (Part number 4352932E), and subtracts them from each other to get the delta Ct (dCt = Ct target – Ct control). This dCt is representative of a relative expression in each sample for the target gene. The delta delta (ddCt) however, is the value needed to compare different samples. This is achieved by comparing the dCt of each value to a chosen calibrator (ddCt = dCt sample – dCt calibrator). Brain was chosen to be the calibrator due to the high expression of FAM57B in that tissue. Due to the exponential nature of PCR that doubles at every Ct increase, the equation "2^{-ddct} =

final relative expression value" is used to express the relative expressions of the target genes in the different tissue samples.

4.2 Protein Expression

4.2.1 Protein Extraction from Tissues

Twelve week old wild-type mice were euthanized using CO_2 asphyxia. The mice were dissected and the following organs were collected in 17x100 mm culture tubes and frozen in liquid nitrogen: kidney, heart, brain, liver, skin (without hair), muscle, tibia without the epiphysis (flushed bone marrow with normal saline), calvaria, and rib cartilage. The samples then were homogenized individually using a Polytron (PT-MR 3000 Kinematica, Switzerland) with 3 ml RIPA (Radio Immuno Precipitation Assay Buffer composed of 150 mM NaCl, 1% NP-40, 0.5% deoxycholate, 0.1% SDS, 50 mM Tris HCl pH 8.0 and EDTA), 3 µl of Protein inhibitor (1:1000) and 60 µl of Phenylmethanesulfonyl Fluoride (1:50); the tibia was first crushed using a pestle and mortar before homogenization. The RIPA buffer was prepared according to the Western Blotting protocol "Western Blotting – A Beginner's Guide" provided on the "Abcam Inc. (Toronto, ON)" website. The samples were then centrifuged at 4° C at 3200 RPM for 20 minutes. The supernatant was transferred to 1 ml eppendorf tubes and the precipitate was disposed of.

4.2.2 Determining Protein Concentration

Protein concentrations were determined using the Bio-Rad (Philadelphia, PA) Protein Assay Dye Reagent with a BSA (Bovine Serum Albumin) standard curve. The absorbance of the standard solutions and the samples were measured at λ = 595 nm using a standard Beckman spectrophotometer. The absorbance of the standard solutions were measured first in succession followed by the samples. The

standard curve was then plotted and the equation of the plot was derived. The concentrations of the samples were deduced from the derived equation.

4.2.3 Developing the FAM57B Antibody

After successfully identifying the potential specific membrane receptor (FAM57Bv2) to 24,25-$(OH)_2$D, a post-doctoral researcher in our laboratory, Laszlo Kupcsik, was able to identify the protein sequence of this receptor. A portion of the receptor's protein sequence was chosen and sent to "Gallus Immunotech Inc." (Fergus, ON) a company that specializes in the production of egg-derived antibodies. The company provided our laboratory with the "Affinity Purified Chicken anti-AGYIVSTSCKHIIIDDQHWLSSAY" that detects all isoforms of FAM57B and is not only specific to FAM57Bv2 along with the blocking peptide. These were used in the western blot and immunohistofluorescence assays detailed below.

4.2.4 Western Blot Analysis

The relative protein expression of FAM57B in different organ tissues of wild-type mice was assessed using western blotting, where the primary antibody used was the specific antibody against FAM57B described above, and the secondary antibody was an Antichicken-IgY.

Two separate western blots were run simultaneously, as one of the membranes was incubated with a solution containing the primary antibody and the blocking peptide while the other was incubated with a solution lacking the blocking peptide.

4.2.5 Electrophoresis

Western blot analysis of the protein samples was performed using the SDS-PAGE method (Sodium Dodecyl Sulfate PolyAcrylamide Gel Electrophoresis) provided in the "Abcam" protocol. The molecular weight of the FAM57B protein is known

to be 31 kDa and thus 10% resolving gel was used for electrophoresis and was prepared according to the protocol using 40% acrylamide, 10% APS (Ammonium persulfate) and TEMED, while 4% stacking gel was prepared using 40% acrylamide, 10% APS and TEMED. The protein samples were prepared using 10 µg of protein, in addition to distilled water and 6x Lamli. These solutions were then boiled for 2-5 minutes and loaded into the wells. The migration buffer used was 1X Tris-glycine and the set voltage was 200 V.

4.2.6 Transfer of Proteins and Staining (Western Blotting)

For the transfer of proteins we used PVDF (Polyvinylidene fluoride, Millipore Ireland Ltd., County Cork, Ireland) membrane and Whatman paper (Whatman International Ltd., Maidstone, England). The transfer buffer used was a solution of 70% distilled water, 20% methanol and 10% 10X Tris-Glycine without SDS. An icepack was added to the chamber and the transfer was done over the duration of 1.5 hours at 100V. Upon completion of the transfer, the membranes were fixed in methanol for 5-10 secs and then left to dry for 5 mins. Blocking was then done by incubating the membranes in a solution of 10% milk on a stirrer for one hour at room temp. The membranes were washed 3 x 5 mins with 1X Tris-buffered saline (TBS) and then the first membrane was incubated with the primary antibody to FAM57B (1:25000) dissolved in 1X TBS, while the other membrane was incubated with a solution containing the primary antibody at a dilution of 1:25000, pre-incubated with the blocking peptide at 200X molar excess. The next day the membranes were washed 3x 10 mins with 1X TBS, and then incubated with the secondary antibody (Anti-chicken IgY) diluted in 1X TBS (1:20000) for 1 hr at room temp. The film was then developed.

4.3 Immunohistofluorescence

Immunohistofluorescence (IHF) was used to detect the location of the FAM57B protein in different mouse organ tissues: brain, kidney and tibia. The methods of preparing paraffin embedded tissues and cryosections will be described below.

4.3.1 Paraffin Embedded Tissues

4.3.1.1 Dehydration

A 12 week old wild-type mouse was euthanized by cervical dislocation, and the brain and both kidneys were obtained and fixed individually in 10% Formalin Solution at 4°C overnight. The next day, dehydration of the tissues was done by incubating them 2 x 1 hr with increasing concentrations of ethanol (70, 80, 95 and 100%). The final 2 steps of dehydration are the incubation of the tissues with xylene 3 x 1 hr, and then with paraffin wax at 56°C (without dimethyl sulfoxide) 2 x 1.5 hrs. The samples were finally embedded into paraffin (with dimethyl sulfoxide) blocks.

4.3.1.2 Tissue Sectioning

Tissue sectioning was prepared using a microtome (Leica RM2255, Concord, ON). The tissues were sliced at a thickness of 5 μm (brain: coronal sections, kidney: saggital sections) and placed on charged adhesion slides. The slides were left to dry overnight at a temperature of 42° C using a glass slide warmer.

4.3.1.3 Deparaffinization

Before proceeding with the staining protocol, the sections had to be deparaffinized. This is essentially the reversal of the dehydration step mentioned above. The slides are placed in a rack and washed in succession starting with

xylene, then xylene 1:1 with 100% ethanol, decreasing ethanol concentrations (100, 95, 70, and 50%) and finally cold tap water. Each wash was done over the duration of 3 minutes.

4.3.1.4 Antigen Retrieval

This step is essential and widely used in formalin-fixed tissues before immunohistofluorescence. During fixation, methylene bridges form which cross-link proteins and thus mask antigen sites. The two methods, heat-mediated and enzymatic, both serve to expose antigenic sites well. We used the heat-mediated method in our experiments.

The antigen retrieval step was performed using the "2100 Retriever" (PickCell Laboratories, Amsterdam, The Netherlands) pressure cooker. The slides were placed in a rack containing sodium citrate buffer (pH 6.0) in the cooker, and antigen retrieval was done according to the protocol found in the manual supplied with the machine. The cooker was left to cool overnight.

4.3.1.5 Immunostaining

After antigen retrieval, the slides were washed with phosphate-buffered saline (PBS) for 3 x 5 mins, and were then washed 2 x 5 mins with 1X TBS plus 0.025% Triton X-100. Blocking of the slides was then done over the duration of 2 hours at room temperature with a solution of 10% normal goat serum with 1% BSA in 1X TBS. After the blocking step, the slides were incubated with the primary antibody at 4°C overnight. For each tissue we used three slides; one slide was used as a negative control (1X TBS and BSA 1%) without the primary antibody, the second was the positive control with the primary antibody (1:250), and the third was incubated with the primary antibody pre-incubated with the blocking peptide at 400X molar excess.

4.3.1.6 Fluorescent Detection

The next day, the slides were rinsed 2 x 5mins with 1X TBS 0.025% Triton with gentle agitation and then incubated with 0.1 % the fluorophore-conjugated (Alexa Fluor 594 goat anti-chicken 2mg/ml) diluted in 1X TBS with 1% BSA for 1 hour at room temperature. The slides were finally stained with 4',6-diamidino-2-phenylindole (DAPI) and were visualized under fluorescence using the fluorescence microscope (Leica DMR, Olympus DP70).

4.3.2 Cryosections

Previously prepared decalcified mouse tibia cryosections cut in the sagittal plane were provided to us by a colleague in our unit, Lisa Lamplugh; the brain and kidney cryosections were prepared and processed by myself as detailed below.

Twelve week old wild-type mice were euthanized by cervical dislocation, and the brain and both kidneys were obtained and fixed individually in 4% Formalin Solution for 10mins. They were then washed 3x 5mins with PBS and cut into 2mm pieces (brain: coronal, kidney: saggital). Next, a cryo-mold was filled with OCT-Tissue-Tek (Sakura Finetechnical Company Ltd., Tokyo, Japan) and placed on crushed dry ice in a Styrofoam box. The samples were left soaking in OCT for a period of 10 minutes to allow good penetration and then stored at -20°C overnight.

The samples were sectioned at a thickness of 5µm using the cryostat (Bright, Model OTF) and placed on previously prepared gelatin coated slides. Staining was then performed as was done to the paraffin embedded slides, but without antigen retrieval.

4.4 Surgical Experimental Design

The *Cyp24a1*$^{-/-}$ mice that were engineered in our laboratory (St-Arnaud et al., 2000) and their wild-type control littermates were used in the following intramedullary surgeries. They were bred and housed in the animal facility of the Shriners Hospitals for Children, Montreal, QC, Canada, with exposure to light for twelve hours per day and twelve hours darkness. Water and regular mouse chow were provided ad libitum. All animal use protocols were approved by the McGill Animal Care and Use committee.

Twelve to 16 week-old *Cyp24a1* deficient mutant mice (St-Arnaud et al., 2000) and wild-type controls were used to perform the IM nailing surgeries. Ten mice were assigned to each of the four different groups: mutants injected with vehicle, mutants injected with 24,25-$(OH)_2$D, wild-types injected with vehicle, and wild-types injected with 24,25-$(OH)_2$D. The mice were sacrificed and the samples were collected at 18, and 28 days post-surgery.

4.4.1 Surgical Procedure (Intramedullary Tibial Nailing)

Several techniques are described in the literature to stimulate fracture repair in rodents, but most of these techniques work better on rat femurs specifically (Holstein et al., 2007; Holstein et al., 2009). Special free weight dropping machines are used in these techniques to stimulate the closed femoral fractures, and immediate post-op radiography is needed to assess the induced fracture (Hiltunen et al., 1993). To avoid the use of weight dropping machines and the need for immediate post-operation radiography to verify the osteotomy, our laboratory was able to devise a modified open-type osteotomy technique to stimulate IM tibial nailing in mice (Husseini, 2011).

Twelve to 16 week-old *Cyp24a1* deficient mice (St-Arnaud et al., 2000) and control wild-types as stated above were used. All operations were performed under aseptic conditions in the procedure room of the animal facility in the

Shriners Hospital for Children, Montreal, Quebec, Canada. The mice were first generally anesthetized using isoflurane gas in a chamber connected to our gas machine, and were kept under anesthesia throughout the full length of the procedure using the same machine. Mice were then weighed on a balance and were subcutaneously injected with 5µl/g of carprofen, 20µl/g of normal saline and 0.05 ml of buprenorphine (0.3mg diluted in 12 ml normal saline); ophthalmic ointment (Neomycin, Polymyxin B sulfates and Bacitracin) was applied to the eyes of the mice to prevent dryness and infection induced by isoflurane. The right leg was shaved using a razor machine starting directly above the knee and down to the ankle, and then prepped with 70% ethanol and 2% chlorhexidine solution. A 3mm vertical skin incision was made above the knee exposing the patellar ligament. The knee joint space was exposed by performing a 2mm medial parapetellar incision using a #11 blade scalpel (Fisher Scientific, Hampton, USA), and a 26G needle was inserted along the direction of the long axis of the tibia through the tibial plateau into the tibial canal. The internal wire core guide of a 25G spinal needle (Quincke 25G 3'' spinal needle, BD #450170, Franklin Lakes, USA) was inserted through the needle and the needle was then removed keeping the wire guide in the tibial canal. The proximal part of the wire was bent at 90 degrees medially and then cut and placed under the patellar ligament avoiding puncture of the ligament. The medial parapetellar incision was closed with a single suture using 6-0 vicryl (Johnson & Johnson, Skillman, USA). Through the same incision, the overlying soft tissue and muscle were bluntly dissected away from the bone at the level of the mid-tibia with 8mm spring micro-scissors (Fine Science Tools #15024-10, Vancouver, Canada). An osteotomy was then performed to stimulate a tibial mid shaft transverse fracture using extra fine Bonn scissors (Fine Science Tools #14084-08, Vancouver, Canada). Using a single 6-0 vicryl suture (Johnson & Johnson, Skillman, USA) the overlying tissue was closed, and analgesia was provided at the surgical site with drops of lidocaine/bupivacaine. Finally, the skin was closed using 2 horizontal mattress sutures (**Figure 13**) (Husseini, 2011). After the surgery the mice were put in a mouse cage placed on a heated pad overnight, and were allowed to ambulate

freely. Six hours post-surgery, the mice were given an injection of 0.05ml buprenorphine subcutaneously, and carprofen (5µl/g of mouse body weight) was administered subcutaneously at 24 hours and 48 hours post-surgery. The animals were closely monitored, and any mice exhibiting signs of severe pain, bleeding, or swelling were humanely euthanized. A total of 160 mice were used for this study.

The rescue experiments were performed in the following manner: The vehicle chosen was propylene glycol (Husseini, 2011). The dose of 24,25-$(OH)_2$D that was administered was 6.7 µg/kg diluted in vehicle; this was an average of the doses used in previous work (Yamate et al., 1994). The mice were administered daily a dose of 50µl volume of 24,25-$(OH)_2$D or vehicle subcutaneously, from the day after the surgery until the date of sacrifice.

Figure 13: Steps of the intramedullary nailing operation. **A.** Insertion of the 26G needle into the tibial canal through the knee joint space. **B.** Insertion of the 25G spinal needle core and suturing of the knee joint. **C.** Induction of the tibial mid shaft fracture with subsequent closure of the surrounding muscle tissue. **D.** Closure of the skin and completion of the surgery. Taken from (Husseini, 2011).

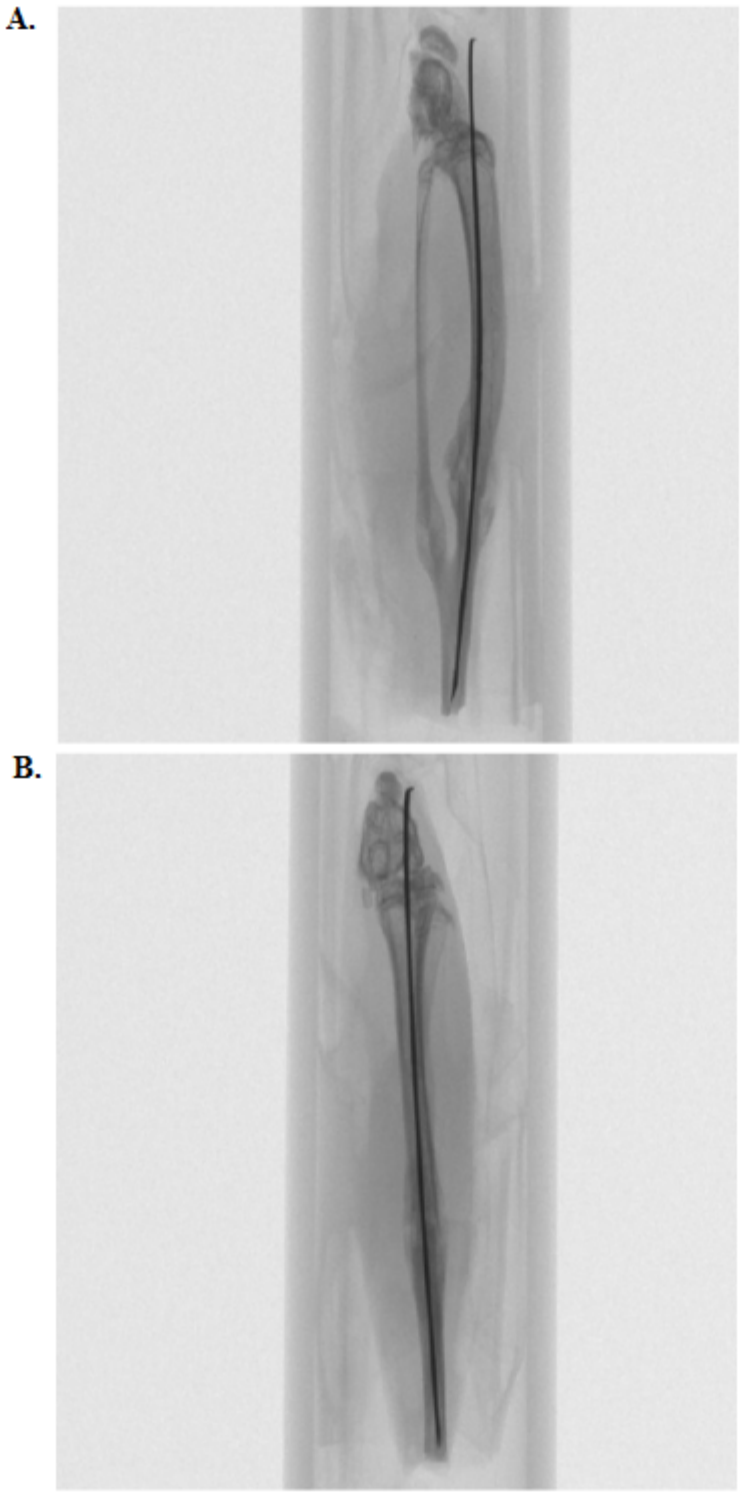

Figure 14: Postoperative views of the inserted tibial nail. **A.** Lateral view. **B.** Anteroposterior view. Taken from (Husseini, 2011).

4.4.2 Sample Collection

The mice from different groups were euthanized in a CO_2 gas chamber at the predetermined time points. The tibiae were disarticulated at the level of the knee and ankle. The overlying skin was completely removed along with the majority of the overlying muscle. The samples were then wrapped in Kimwipe (Kimtech Science, Kimberly Clark Inc., Mississauga, ON) paper and stored in PBS at -40°C pending biomechanical testing.

4.4.3 Three Point Bending

The samples were left at room temperature to thaw overnight before performing the three point bending test. The kimwipe was carefully removed off the sample and the intramedullary nail was carefully pulled out using a needle holder. The sample was then broken at the fracture site using the three point bending machine, and the data generated were recorded and analyzed to give the stiffness (N/mm) and the force (N) needed to break each sample. The samples collected were tested in our laboratory using our three point bending machine (Instron, Norwood, MA) (**Figure 15**).

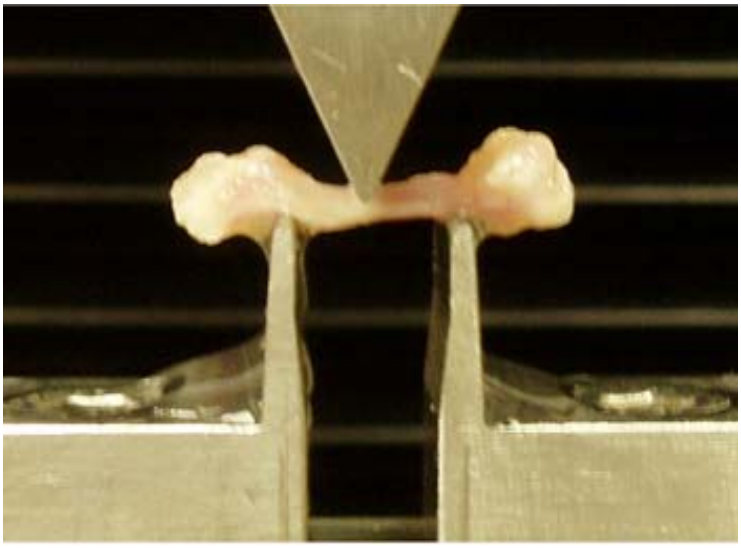

Figure 15: An example of mouse femur loaded on a three-point bending machine. Taken from: www.mc.vanderbilt.edu

4.5 Statistical Analysis

To analyze the numerical data generated from the biomechanical testing of the tibia samples, we used the statistical program prism 5.0 (GraphPad software Inc., La Jolla, USA). Two-way ANOVA with post-hoc Newman-Keuls Comparison analysis of the Log transformation of the values was used to compare the different groups. A p value of <0.05 was considered to be significant.

5. Results

5.1 FAM57B

5.1.1 qRT-PCR results: mRNA Expression of *Fam57b* and *Fam57bv2*

mRNA expression of total *Fam57b* and *Fam57bv2* in different organ tissues of wild-type mice were measured using qRT-PCR. The graphs below represent the relative expression of either of the two transcripts from the gene in the different samples compared to the calibrator, brain.

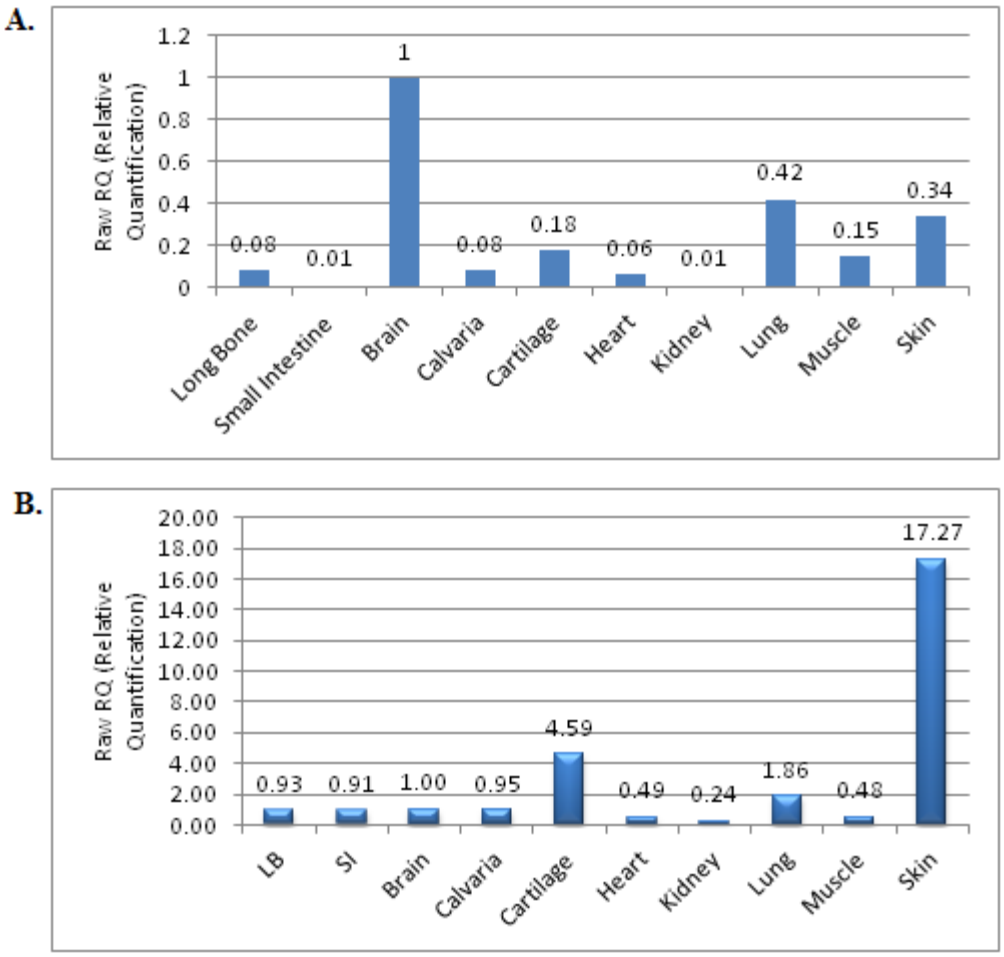

Figure 16: A. Relative mRNA expression of *Fam57b* and **B.** Relative mRNA expression of *Fam57bv2* in WT mice.

It can be seen that the mRNA expression of total *Fam57b* was highest in brain tissue compared to the rest. The other tissues all express the gene at much less relative quantities (**Figure 16A**). Interestingly though, looking at the mRNA expression of *Fam57bv2*, we observe that different organ tissues express this gene at much higher concentrations relative to brain. In fact skin and cartilage tissue show the highest expression of variant 2 (**Figure 16B**). This data is interesting as it shows that *Fam57bv2* is highly expressed in a tissue that participates in fracture healing (cartilage), and in a tissue that undergoes lots of repair (skin).

5.1.2 Western Blot Analysis Results

Western blot analysis was used to assess FAM57B protein expression in different organ tissues of wild-type mice using the FAM57B antibody and blocking peptide.

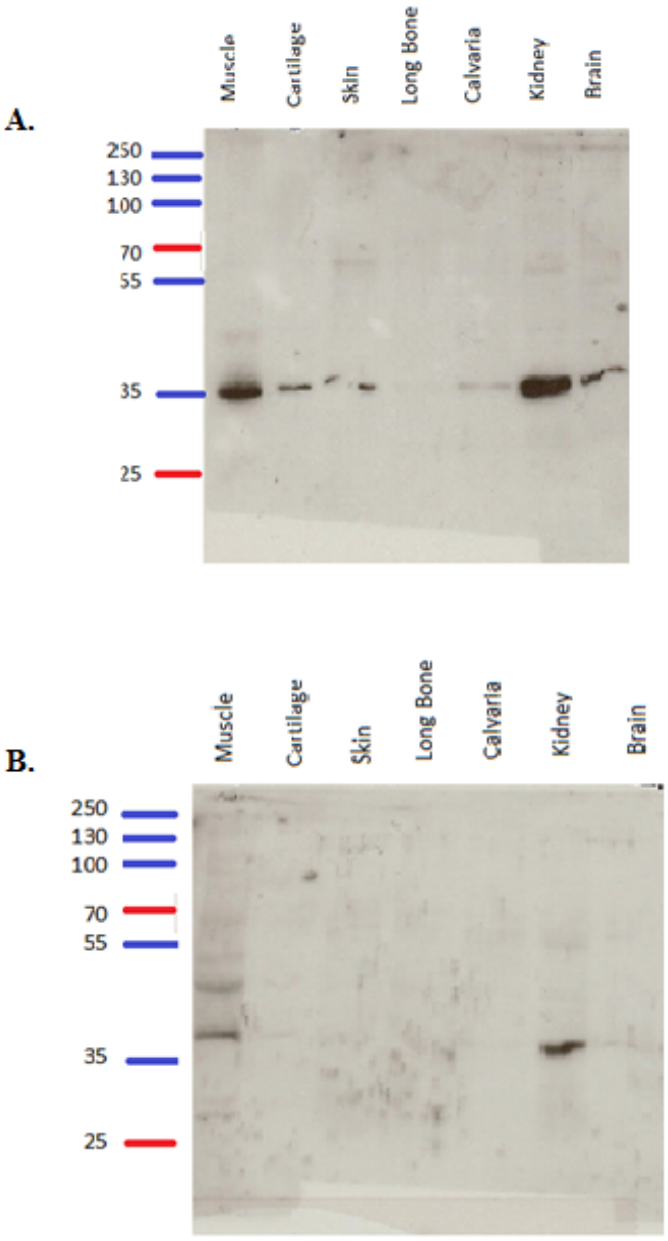

Figure 17: A. Western Blot analysis of FAM57B in different organ tissues. **B.** Western Blot analysis of FAM57B + Blocking Peptide in different organ tissues.

The antibody used here is not specific to FAM57Bv2 but is able to detect all isoforms of FAM57B, and thus in the blots above, the antibody is detecting all isoforms of FAM57B. Tissues assayed including liver (data not shown) express a band at ~35 kDa which corresponds to the molecular size of the FAM57B protein. The tissues that express FAM57B the most are the kidney, brain and muscle, although the gel was not controlled for loading. Looking at the second western blot **(Figure 17B)**, we see in almost all of the organ tissues that the band has disappeared; this is due to the effects of the blocking peptide on the FAM57B antibody. Since the blocking peptide used is known to be specific to the antibody, the results suggest that the bands seen in the first blot are truly representative of FAM57B. Since loading of the proteins was not controlled for, the reason for the high intensity bands seen in the kidney and muscle columns in the first blot (**Figure 17A**) is that there was more protein loading in those wells compared to the rest. This resulted in incomplete disappearance of those bands in the second blot (**Figure 17B**). We anticipate that if more blocking peptide had been added to the blot, the high intensity bands would disappear completely.

5.1.3 Immunohistofluorescence

IHF is a method commonly used to demonstrate the presence and location of proteins in tissue sections. Even though it is quantitatively less sensitive than Western Blotting or ELISA, it allows the researcher to identify the location of the protein in the context of intact tissue. Since the primary antibody used in this method is usually highly specific to its protein, it will only bind to the protein of interest in the tissue section. After this step, a secondary antibody that has a flurophore conjugated to it, will allow visualization of the protein-Antibody complex using fluorescence microscopy. We have used this method to further identify FAM57B in paraffin embedded tissues, and tissue cryosections.

5.1.3.1 Paraffin Sections

Figure 18 shows the results of immunofluorescence detection of FAM57B in paraffin sections from fixed brain tissue. Background staining in the absence of primary antibody was low (panel A). Incubation with the primary antibody yielded a diffuse signal (panel B) that was partially blocked upon incubation of the antibody with the immunizing peptide (panel C). The signal seen in panel B most likely represents specific staining as it diminishes upon peptide blocking; however, the diffuse signal does not allow identifying expressing cells unambiguously. A number of antigen retrieval and incubation conditions were tried without improving the specific signal (data not shown). Moreover, we could not detect a specific signal in paraffin sections from kidney, where the protein is abundantly expressed (data not shown, and **Figure 17A**). We conclude that the antibody does not work very well for immunodetection in fixed tissue embedded in paraffin.

A.

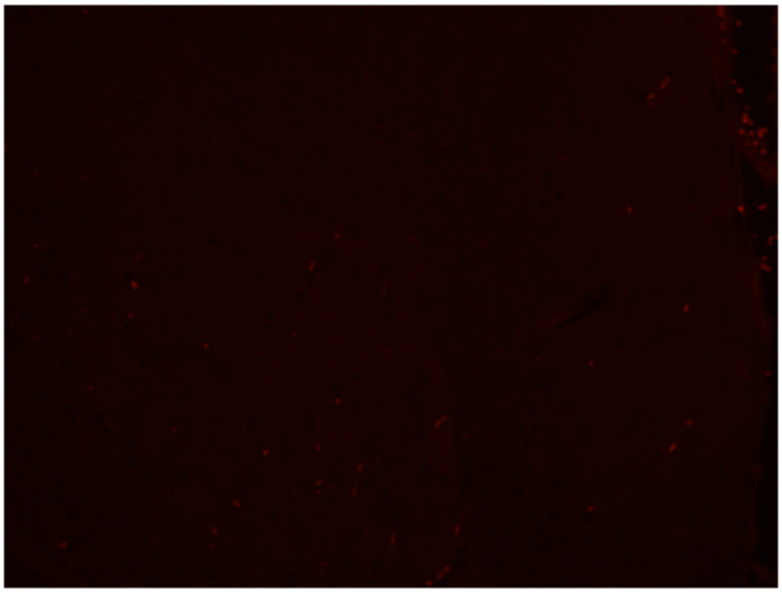

B.

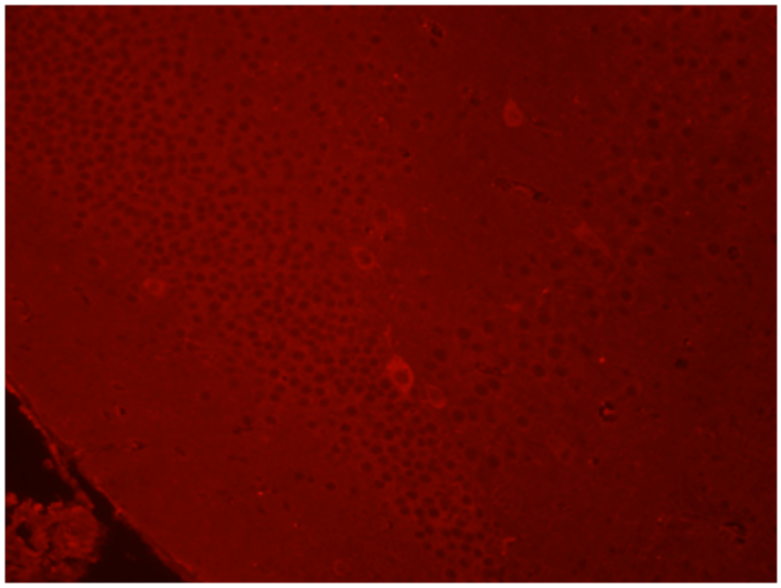

C.

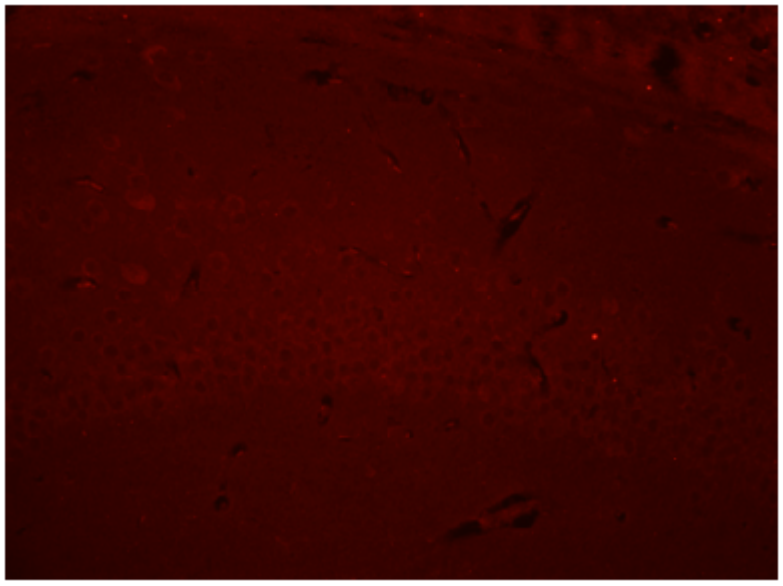

Figure 18: Brain paraffin section **(A)** without antibody, **(B)** with antibody, and **(C)** with antibody plus blocking peptide.

5.1.3.2 Cryosections

Figures 19 and **20** show immunofluorescent detection of FAM57B in cryosections from kidney (**Figure 19**) or joint tissue (**Figure 20**). In each case, background staining was low (**Figure 19A** and **Figure 20A**) and we could detect a specific signal (panels B of each figure) that was blocked upon preincubation with the immunizing peptide (**Figure 19C** and **Figure 20C**). Cryosectioning does not yield good histology, especially of soft tissues, and it remains difficult to ascertain which structure/cell type expresses FAM57B in kidney. However, the joint cryosection can be oriented to identify the distal and proximal portions of the bones as well as the meniscus cartilage. The specific staining for FAM57B was detected in the meniscus cartilage tissue (**Figure 20B**). This result combined with the mRNA expression profiling of *Fam57bv2* that shows high transcript levels in cartilage (**Figure 16B**) suggests that the antibody detects the FAM57B2 protein isoform in chondrocytes from cartilage. This is a cell type that contributes to fracture repair through endochondral ossification and is a relevant site of expression for a role of the FAM57B2 protein in transmitting the signal from 24,25-$(OH)_2$D during fracture healing.

A.

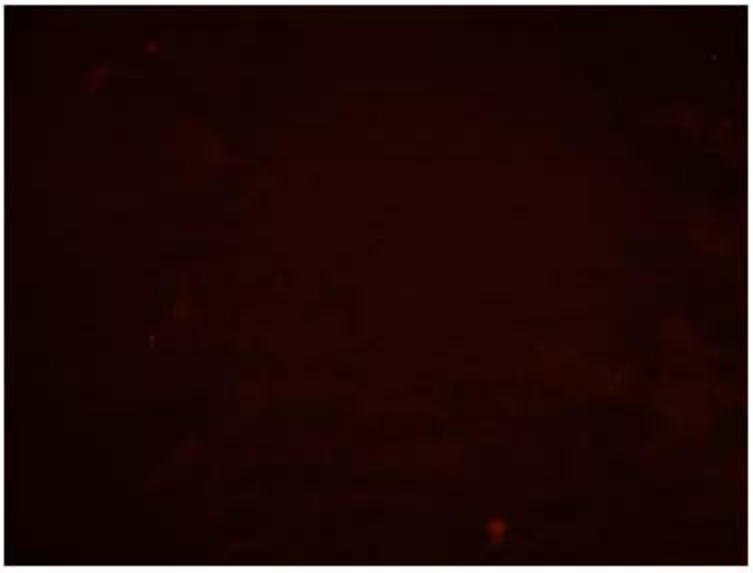

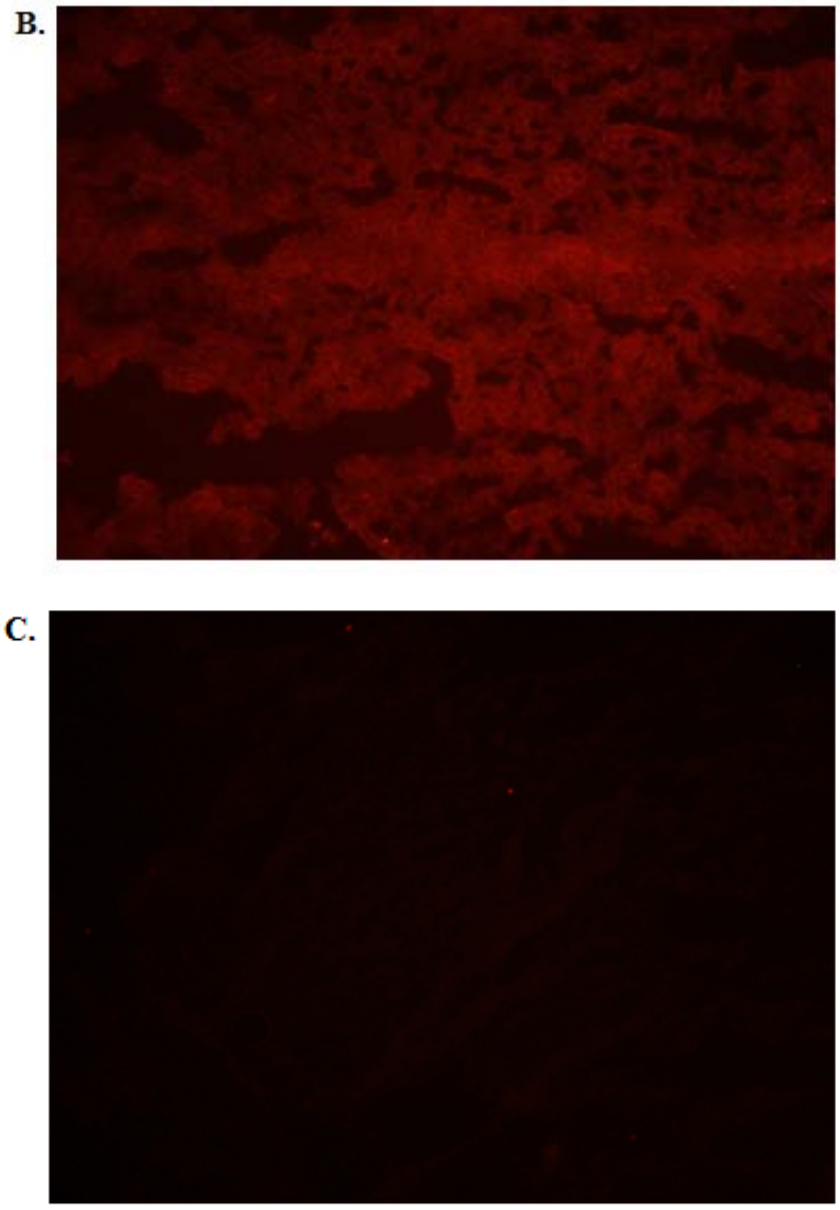

Figure 19: Kidney cryosection without antibody **(A)**, with antibody **(B)**, and with antibody plus blocking peptide **(C)**.

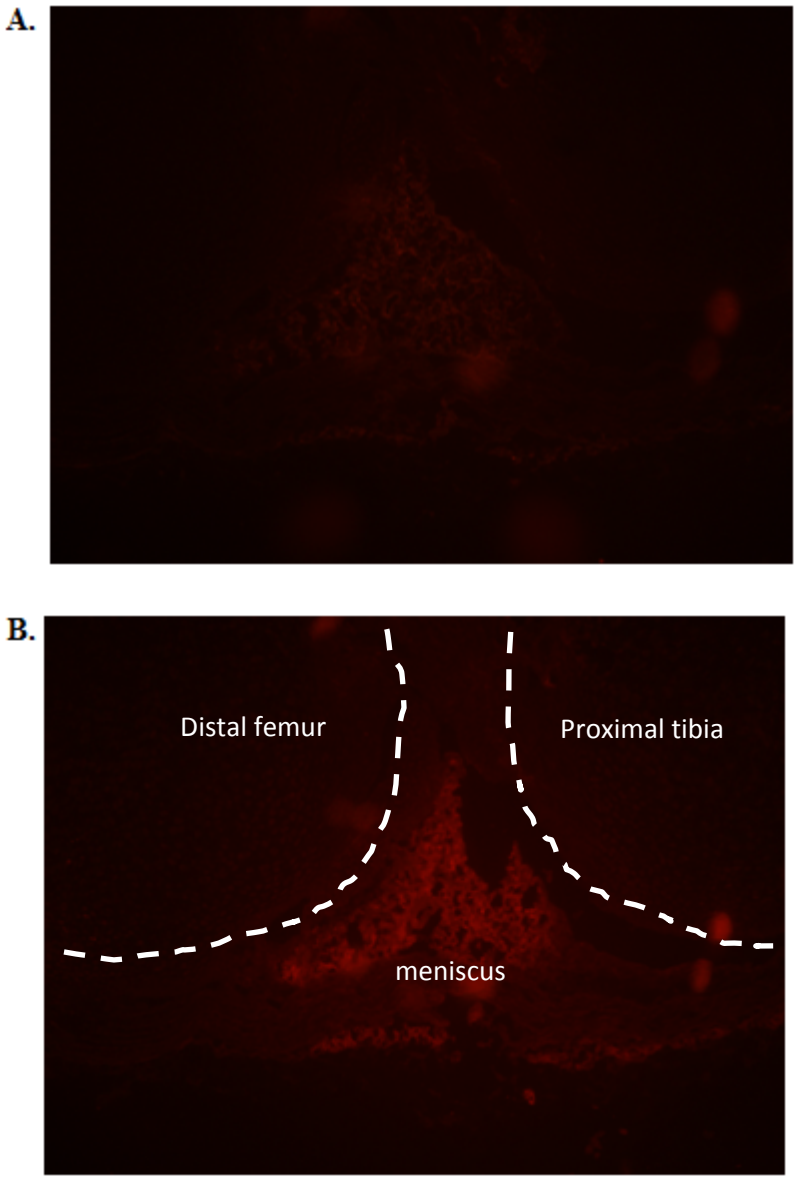

Figure 20: Tibia cryosection without antibody **(A)** and with antibody **(B)**.

5.2 Intramedullary Nailing Experiment

As stated in the above Material and Methods section, we sacrificed the operated mice at two different time points. The time points corresponded to post-operation days 18 and 28, and the biomechanical parameters of the samples (stiffness and force needed to break) were measured at these time points These time points were based on previous work that showed that the differences in bone formation between the mutant mice and wild-type mice were most evident by day 18 and normalized by day 28 (**Figure 9**) (Husseini, 2011). The results in this section are presented for each gender at both time points.

5.2.1 Day 18 post-operation

Three – point bending: Stiffness

Gender: male

18 days post-surgery

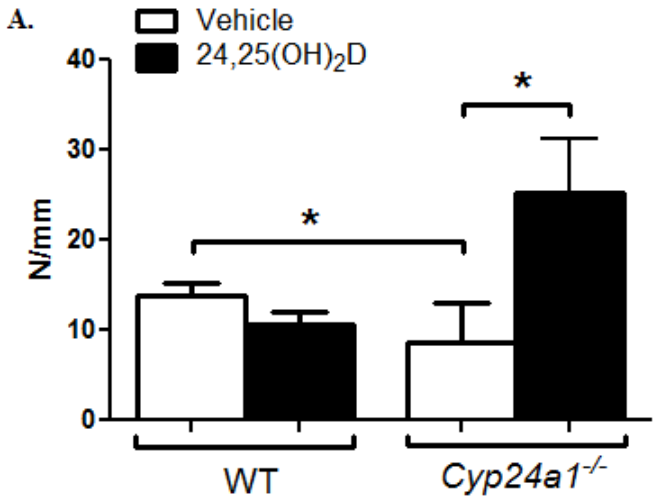

Three – point bending: Force to break

Gender: male

18 days post-surgery

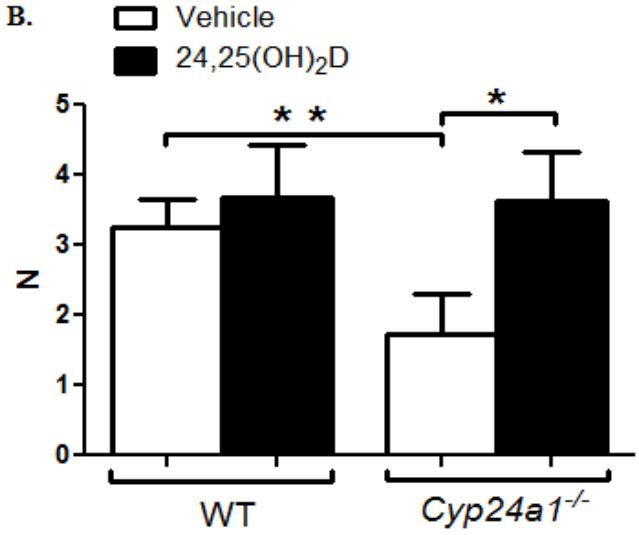

Figure 21: Column bar graph of the stiffness **(A)** and force to break **(B)** of male samples at 18 days post-operation.

Three – point bending: Stiffness

Gender: Female

18 days post-surgery

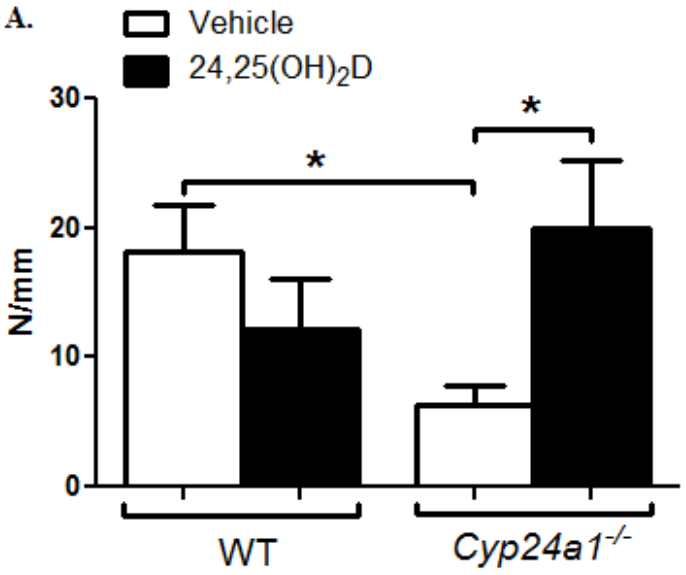

Three – point bending: Force to break

Gender: Female

18 days post-surgery

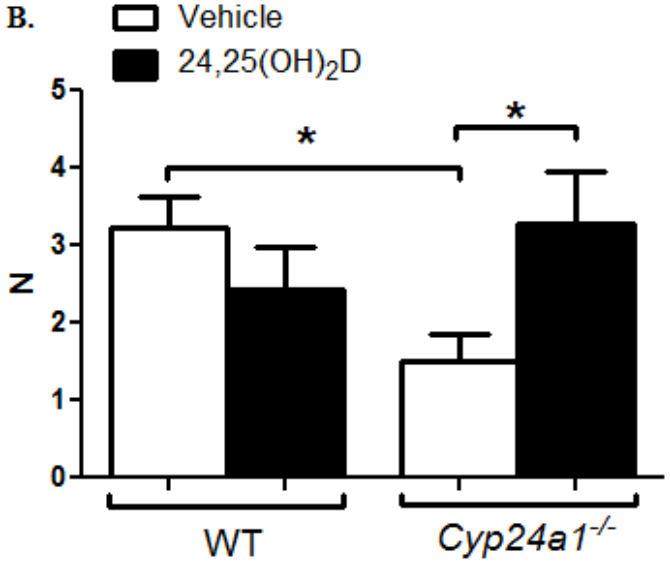

Figure 22: Column bar graph of the stiffness **(A)** and force to break **(B)** of female samples at 18 days post-operation.

5.2.2 Day 28 post-operation

Three – point bending: Stiffness

Gender: Male

28 days post-operation

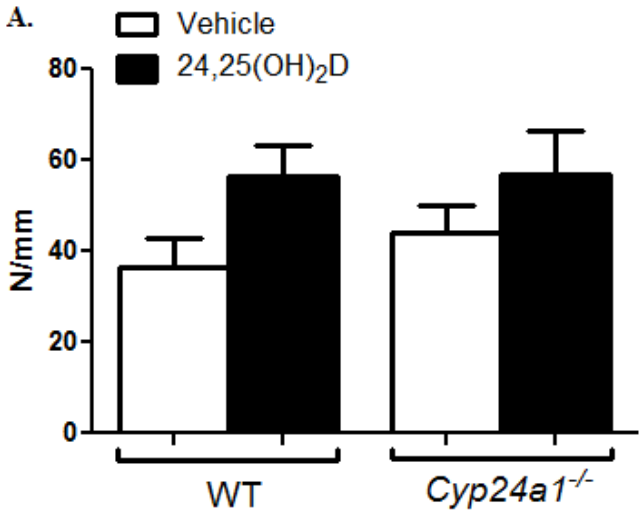

Three – point bending: Force to break

Gender: Male

28 days post-operation

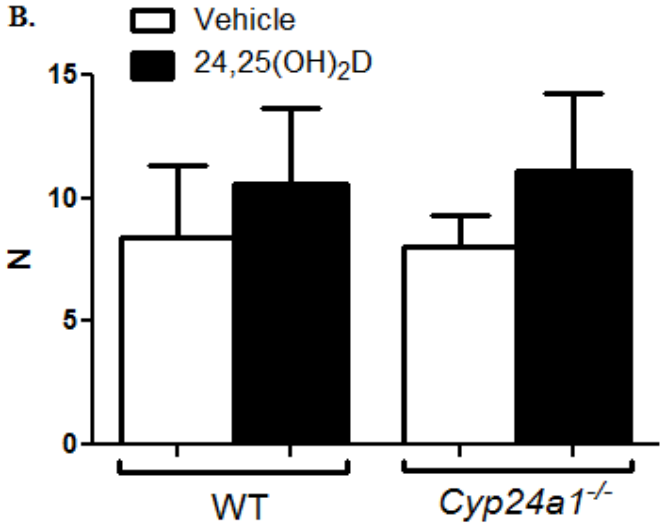

Figure 23: Column bar graph of the stiffness **(A)** and force to break **(B)** of male samples at 28 days post-operation.

Three – point bending: Stiffness

Gender: Female

28 days post-surgery

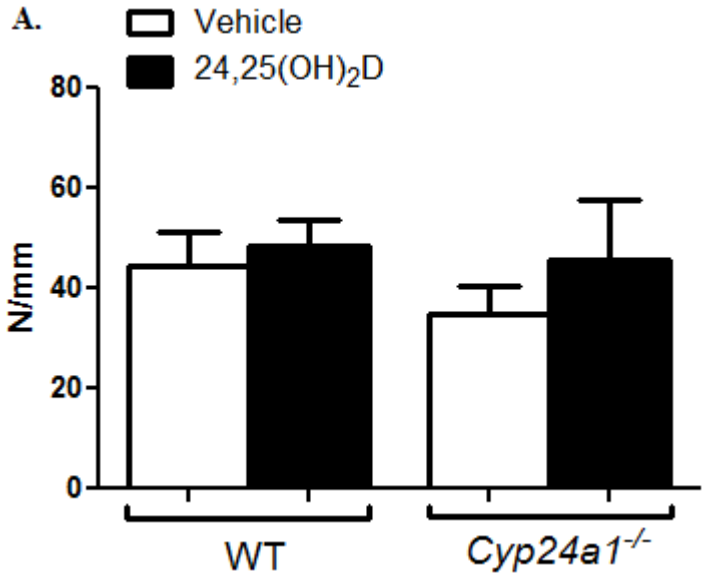

Three – point bending: Force to break

Gender: Female

28 days post-surgery

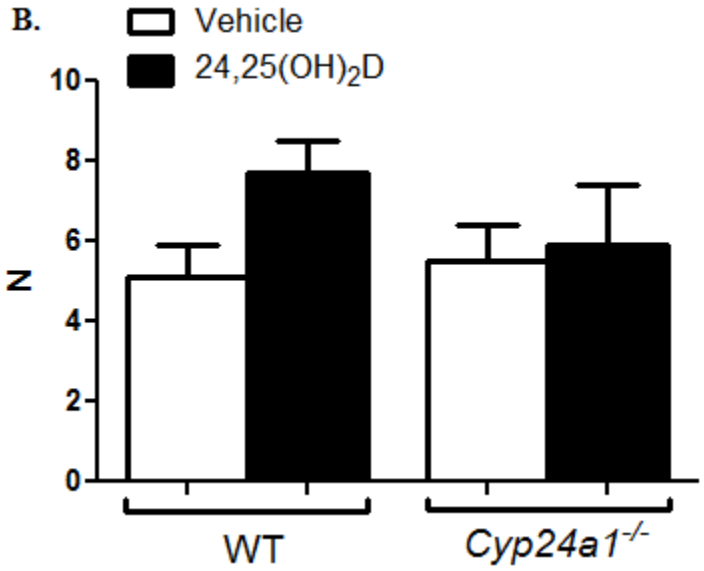

Figure 24: Column bar graph of the stiffness **(A)** and force to break **(B)** of female samples at 28 days post-operation.

As measured at day 18 post-operation, the calluses of the untreated mutant males (vehicle) had significantly lower stiffness (**Figure 21A**) compared to their wild-type littermates, and required less force to break (**Figure 21B**). These differences were rescued with the administration of exogenous 24,25-$(OH)_2$D. The calluses of the mutant mice given 24,25-$(OH)_2$D had significantly superior biomechanical properties compared to the mutants given vehicle, and were similar to the their wild-type littermates. The differences seen were not gender-specific, as we obtained similar results in the female group (**Figure 22**). Therefore we can conclude that 24,25-$(OH)_2$D helps in optimizing fracture healing at an early stage of repair in all genders.

The differences in the biomechanical parameters seen at day 28 post-operation among the four different groups were not found to be statistically significant. This is in line with previous results obtained in our laboratory, showing that there are no differences in callus formation towards the end of fracture healing (Husseini, 2011). However, there was no detrimental effect of 24,25-$(OH)_2$D on wild-type calluses. In fact, it can be argued that the results show a trend that might be indicative of a beneficial effect of 24,25-$(OH)_2$D on WT mice calluses (**Figure 23**, **Figure 24)**. The effect could have reached statistical significance if we had used larger cohorts.

These results suggest that 24,25-$(OH)_2$D plays a significant role in optimizing mammalian fracture healing. Administration of exogenous 24,25-$(OH)_2$D rescues the delay in fracture healing observed in *Cyp24a1*-deficient animals. This replacement therapy is effective in both genders.

6. Discussion

We set out to examine the expression pattern of the mRNA and protein for a putative receptor binding the vitamin D metabolite, 24,25-$(OH)_2$D. We also measured the effect of treatment with 24,25-$(OH)_2$D on the biomechanical properties of healing bones. To perform this study, we have used the *Cyp24a1* deficient mice that were previously engineered in our laboratory (St-Arnaud et al., 2000), as well as several organ tissues extracted from wild-type mice.

The CYP24A1 enzyme and its metabolite 24,25-$(OH)_2$D have been extensively studied for quite some time, and the results have been a matter of ongoing debate. Studies and experiments first performed led to the interpretation that this metabolite was a mere degradation product and did not possess biological activity (Tanaka et al., 1979; Ameenuddin et al., 1982; Jarnagin et al., 1983). When scientists began to look at different physiological functions for this metabolite, they found that it plays a beneficial role in bone health and mineral content, as well as strength and maturity when administered at pharmacological concentrations (Nakamura et al., 1992; Nakamura et al., 1992; Nakamura et al., 1992). More convincing evidence for identifying a specific role for 24,25-$(OH)_2$D distinct from 1,25-$(OH)_2$D was obtained by studying fracture repair in chicken. Studies were able to show that there was an increase in CYP24A1 activity with accompanying increase in 24,25-$(OH)_2$D serum levels after tibial fracture in chicken (Seo et al., 1997), and that the addition of 24,25-$(OH)_2$D to the diet of these chicken alone was able to achieve optimal bone repair with subsequent superior biomechanical parameters compared to chicken fed 1,25-$(OH)_2$D alone (Seo et al., 1997). Our laboratory was successful in developing a mouse model deficient for *Cyp24a1* that served as a valuable tool to study the role of 24,25-$(OH)_2$D in mammalian fracture repair. These mice were studied using two different surgical techniques that yielded interesting results.

The first set of experiments performed involved subjecting mutant mice and their wild-type littermates to tibial fractures, and then stabilizing these fractures using

an external fixator. Using bone histomorphometry, the bone volume and callus structures of these mice were examined at days 14 and 21 post osteotomy. The wild-type mice calluses had hyaline cartilage and woven bone, indicative of normal fracture healing and repair; interestingly, the mutant mice showed no such features and exhibited smaller and very poorly organized calluses. When 1,25-$(OH)_2D$ was administered to these mutant mice, there was no improvement in callus size and quality; however, with the administration of 24,25-$(OH)_2D$ the calluses of the mutant mice increased in size and showed features of normal histology similar to wild-type calluses (Naja, 2008).

The second set of experiments performed in our laboratory further supported these results using a different surgical modality. A modified open osteotomy with intramedullary nailing procedure was developed in our laboratory that successfully mimics endochondral ossification. Using this surgical technique, mutant mice and their wild-type littermates were subjected to tibial fractures and the resulting calluses were studied using micro-CT. In line with the results of the first set of experiments done, the callus sizes of the mutant mice were significantly smaller at days 10 and 18 when compared to the wild-type calluses; however, at days 21 and 28 the mutant calluses reached the same size as the wild-type calluses (**Figure 9**). Furthermore, injecting the mutant mice with exogenous 24,25-$(OH)_2D$ resulted in the calluses attaining a size similar to the wild-type control (vehicle) mice at days 10, 18, 21 and 28 (Husseini, 2011). These results, in concordance with the results of the first set of experiments show a highly important role for 24,25-$(OH)_2D$ and not 1,25-$(OH)_2D$ in optimizing fracture repair and speeding up the healing process in the early stages.

In this study we attempted to further validate the role of 24,25-$(OH)_2D$ in optimizing fracture repair by assessing the biomechanical properties of the mutant mice calluses and the calluses of their wild-type littermates, using the modified open osteotomy technique with intramedullary nailing that was developed in our laboratory. With the knowledge that the calluses of the mutant and wild-type mice exhibited differences with respect to size and morphology at day 18 that were not

seen at day 28 post-operation, we used these two distinct time points to assess the stiffness of the different calluses, and the force needed to break the healing bones. At day 18, the male and female mutant calluses had significantly inferior biomechanical properties compared to the wild-type control calluses. When mutant male and female mice were given exogenous 24,25-$(OH)_2D$, they attained similar biomechanical properties as the wild-type controls (even more superior in the males), and those properties were significantly superior from the calluses of the mutant mice given vehicle.

At day 28, when healing is complete, we did not measure statistically significant differences between groups. These results are in line with the previous results from our laboratory that show a delay in fracture healing in *Cyp24a1*$^{-/-}$ mice that is recovered upon full healing. This may suggest that 24,25-$(OH)_2D$ serves as a catalyst for this process but is not a vital metabolite where its absence will fully impair mammalian fracture repair. It should be noted that in both genders, 24,25-$(OH)_2D$ did not have a detrimental effect on the wild-type mice; in fact, we notice that at day 28 post-operation there could be a potentially beneficial effect of 24,25-$(OH)_2D$ on the calluses, as the wild-type and mutant mice supplemented with this metabolite showed superior properties compared to the ones given vehicle. One of the reasons why these differences did not reach statistical significance could be due to the sample size number, and thus had our sample size been larger we could have attained statistical significance.

We also assessed the biomechanical properties of non-operated wild-type and mutant mice tibiae (data not shown). The results obtained were very similar and showed no differences at all between the two groups in both genders; in addition, there were no variations between the different samples of the same genotype. These results show that 24,25-$(OH)_2D$ plays an essential role in fracture repair but has no major effects on steady state bone biomechanics.

The results of the surgical part of this work are in line with the results of the previous two studies performed. The first study utilized a miniature Ilizarov apparatus that served as an external fixator to study the callus formation of

fractured tibiae. The histology of the calluses of the mutant mice was then compared to the calluses obtained from WT mice (Naja, 2008). The second study adopted the modified open osteotomy with subsequent intramedullary nailing of the tibia technique to further compare callus formation between mutant mice and WT mice using micro-CT (Husseini, 2011). Using this surgical technique, in the third study we compared the biomechanical parameters of repaired bones in mutant mice compared to the ones of WT mice. We were able to show through three different studies, using two different surgical techniques, and by measuring different outcomes that the absence of 24,25-$(OH)_2$D causes a delay in fracture healing that can be rescued with the exogenous administration of this metabolite. Combined, these studies firmly show that 24,25-$(OH)_2$D plays a crucial and essential role in speeding up and optimizing mammalian fracture healing, but it is not vitally important where its absence would result in a failure of fracture repair.

The search for a distinct specific receptor to 24,25-$(OH)_2$D has long been ongoing but without much promising results. Many groups have attempted to localize such a receptor and have suggested different locations. These efforts were descriptive and never led to the isolation and characterization of a molecular clone (Canterbury et al., 1978; Chertow et al., 1980). The *Cyp24a1* deficient mouse served as a valuable model to try to identify such a specific receptor, and our laboratory was successful in characterizing FAM57Bv2 (an isoform of FAM57B) as a membrane receptor that binds 24,25-$(OH)_2$D and not 1,25-$(OH)_2$D in a specific and saturable manner. The identification of FAM57Bv2 as a receptor to 24,25-$(OH)_2$D allowed for the development of an antibody (with its blocking peptide) and primers that were used in this work to further characterize the location of this receptor in wild-type mice. We performed mRNA and protein analysis on different organ tissues of the wild-type mouse.

Our qRT-PCR results showed that brain has the highest expression of *Fam57b* whereas skin and cartilage show the highest expression of *Fam57bv2*. On one hand, this does not come as a complete surprise, as skin is an organ that is continuously undergoing repair and thus it is not a shock that FAM57Bv2, which

we believe is involved in mammalian fracture repair, could also be involved in the repair of different organs in the body. Our laboratory is currently in the process of developing a *Fam57b*$^{-/-}$ mouse that might serve as a valuable model to study the effects of FAM57B on the repair of different organs. The potential putative role of FAM57B in skin repair can be further evaluated through wound healing studies between WT and *Fam57b*$^{-/-}$ mice. Such an experiment could involve performing skin punch biopsies on both the mutant and WT mice and then comparing the respective rates of wound healing. The results of these studies can be used to further characterize the role of 24,25-$(OH)_2$D and FAM57B in the different organ systems.

On the other hand, *Fam57bv2* has been recently shown to be highly expressed in adipocyte tissue where it regulates adipocyte differentiation through ceramide synthesis; thus FAM57Bv2 acts as a ceramide synthase and is involved in the *de novo* synthesis of ceramide (Yamashita-Sugahara et al., 2013). The reason behind the high expression of *Fam57bv2* that we found in skin could be due to the presence of fat on the skin sample, and that the high expression was actually in the adipocytes and not skin cells. However, it has been recently shown that ceramide is involved in extracellular matrix (ECM) mineralization and that the lack of ceramide causes decreased mineralization. *Smpd3* is the gene that encodes neutral sphingomyelinase 2 (nSMase2), a membrane bound enzyme that cleaves sphingomyelin to generate the lipid second messenger ceramide (Khavandgar et al., 2011). A mutation (*fragilitas ossium* or *fro*) that replaces the last 33 amino acids of nSMase2 results in a significant reduction of total neutral sphingomyelinase activities in the tissues of these *fro/fro* mice (Stoffel et al., 2005; Stoffel et al., 2007), which resulted in a subsequent decrease in ceramide levels. These mice had significantly decreased mineralization of the ECM and the skeleton, with significantly increased osteoid volume over total bone volume compared to WT littermates (Khavandgar et al., 2011). Thus identifying ceramide as an important regulator of skeletal mineralization (Khavandgar et al., 2011) and characterizing FAM57Bv2 as a ceramide synthase (Yamashita-Sugahara et al.,

2013) suggest that FAM57Bv2 could play a highly important role in mineralization during fracture healing.

Studying the phenotype of mice lacking *Fam57b* should be able to add more knowledge on what is the role of FAM57B in mineralization and fracture repair. Because of the relationship between a ligand and its receptor, we anticipate that the *Fam57b* knockout mouse that is being currently developed would have the same phenotype as the *Cyp24a1* deficient mouse. In other words, similar to VDDR, where mutations in either the activating enzyme (Glorieux et al., 2011) or the receptor (Malloy et al., 2011) yield the same phenotype with different biochemical parameters, we expect a mouse lacking FAM57B to have a phenotype similar to the one seen in the mouse lacking the CYP24A1 enzyme, but with increased levels of 24,25-$(OH)_2$D. Potential studies on such a mouse strain would be similar to what was performed on the *Cyp24a1*$^{-/-}$ mouse in relation to fracture repair. We hope that the fracture calluses of the mutant mice would have the same histological and biomechanical parameters as the calluses of our current mutant mouse strain; these results would be crucial to further validate the highly important role of CYP24A1 and 24,25-$(OH)_2$D in speeding up mammalian fracture repair.

Our western blot analysis showed expression of FAM57B in all of the tissues studied, and the bands visualized were successfully eliminated when the blocking peptide was added to the blot. The main purpose of our western blot analysis was not to assess FAM57B quantitatively, but qualitatively, and thus loading was not fully controlled for. It is imperative in the future to study and assess quantitatively the protein expression of FAM57B in wild-type mice. In addition, we performed immunohistofluorescence analysis on both paraffin embedded and cryosections of brain, kidney and tibia. We believe we were most successfully able to detect FAM57B using kidney and tibial cryosections. The fluorescence detected was successfully diminished when the blocking peptide was added to the sections thus showing that what was detected was truly FAM57B. We have exhausted all efforts by using different types of antigen retrieval, buffers and concentrations of

antibody and blocking peptide and were not able to achieve better images than what was presented in this work, which allowed us to characterize the location of FAM57B in the tibial section in the articular cartilage of the meniscus. With respect to the brain paraffin sections and kidney cryosections, we were not able to fully characterize the location of the protein but have shown that it is present and detectable by our antibody. Perhaps the next step would be to perform these experiments on the *Cyp24a1* mutant mice and assess the mRNA and protein expression of the receptor in those tissues. We would expect to see higher mRNA and protein expression in the mutant tissues than what we obtained in this study; this would allow us to further characterize and quantify FAM57B as a specific receptor to 24,25-$(OH)_2$D.

Uncovering a highly important and crucial role for CYP24A1 and 24,25-$(OH)_2$D in optimizing mammalian fracture repair has several important clinical implications. One implication would be the use of this metabolite as a supplement by patients with long bone fractures to speed up and optimize their healing. It is known that patients with orthopedic fractures are at high risk of infection after surgery (Dellinger E, 1988) which is accompanied by an increase in hospitalization and morbidity and mortality (Kathryn B. Kirkland et al., 1999); it would seem very beneficial to speed up fracture healing with the aim of decreasing hospitalization after surgery and the subsequent risk of infection. It could be argued that supplementation with 24,25-$(OH)_2$D is unnecessary since it is a metabolite resulting from the catabolic breakdown of 25-(OH)D, and that the majority of the population probably has adequate vitamin D levels due to high sun exposure and dietary intake. In reality, very few foods naturally contain vitamin D and the ones fortified with vitamin D are not enough to satisfy a child or an adult's biological requirements; in addition, many people do not get adequate sun exposure and thus vitamin D deficiency is now considered to be a pandemic, causing rickets in children and increasing the risk of osteopenia, osteoporosis and fractures in adults (Holick et al., 2008). Therefore, 24,25-$(OH)_2$D supplementation would serve great benefits to people subjected to fractures in a population whose majority is vitamin D deficient. Increasing awareness about

vitamin D deficiency and educating the public on proper intake and supplementation should also be an important aim in the future.

In conclusion, we firmly believe that the results obtained in our studies have contributed to the field of vitamin D and fracture repair, and have shown that the enzyme CYP24A1 and its metabolite 24,25-$(OH)_2$D play a highly important role in optimizing mammalian fracture repair.

7. References

Adams, J. E. (2011). Chapter 49 - Radiology of Rickets and Osteomalacia. Vitamin D (Third Edition). F. David, J. W. Pike, J. W. P. John S. AdamsA2 - David Feldman and S. A. John. San Diego, Academic Press**:** 861-889.

Aho, A. J. (1966). "Electron microscopic and histological observations on fracture repair in young and old rats." Acta Pathol Microbiol Scand: Suppl 184:181-195.

Ai-Aql, Z. S., A. S. Alagl, D. T. Graves, L. C. Gerstenfeld and T. A. Einhorn (2008). "Molecular mechanisms controlling bone formation during fracture healing and distraction osteogenesis." J Dent Res **87**(2): 107-118.

Ameenuddin, S., M. Sunde, H. F. DeLuca, N. Ikekawa and Y. Kobayashi (1982). "24-hydroxylation of 25-hydroxyvitamin D3: is it required for embryonic development in chicks?" Science **217**(4558): 451-452.

Askew, F. A., R. B. Bourdillon, H. M. Bruce, R. G. C. Jenkins and T. A. Webster (1930). "The Distillation of Vitamin D." Proceedings of the Royal Society of London. Series B, Containing Papers of a Biological Character **107**(748): 76-90.

Attie, M. F., J. R. Gill, Jr., J. L. Stock, A. M. Spiegel, R. W. Downs, Jr., M. A. Levine and S. J. Marx (1983). "Urinary calcium excretion in familial hypocalciuric hypercalcemia. Persistence of relative hypocalciuria after induction of hypoparathyroidism." J Clin Invest **72**(2): 667-676.

Beckman, M. J., P. Tadikonda, E. Werner, J. Prahl, S. Yamada and H. F. DeLuca (1996). "Human 25-hydroxyvitamin D3-24-hydroxylase, a multicatalytic enzyme." Biochemistry **35**(25): 8465-8472.

Buckwalter, J. A. (1996). "Effects of early motion on healing of musculoskeletal tissues." Hand Clin **12**(1): 13-24.

Burgos-Trinidad, M. and H. F. DeLuca (1991). "Kinetic properties of 25-hydroxyvitamin D- and 1,25-dihydroxyvitamin D-24-hydroxylase from chick kidney." Biochim Biophys Acta **1078**(2): 226-230.

Burr, D. B., Turner, C. H. (2003). Biomechanics of Bone. Primer on the Metabolic Bone Diseases and Disorders of Mineral Metabolism. M. Favus. Washington DC, American Society for Bone and Mineral Research.

Cali, J. J. and D. W. Russell (1991). "Characterization of human sterol 27-hydroxylase. A mitochondrial cytochrome P-450 that catalyzes multiple oxidation reaction in bile acid biosynthesis." J Biol Chem **266**(12): 7774-7778.

Canterbury, J. M., S. Lerman, A. J. Claflin, H. Henry, A. Norman and E. Reiss (1978). "Inhibition of parathyroid hormone secretion by 25-hydroxycholecalciferol and 24,25-dihydroxycholecalciferol in the dog." J Clin Invest **61**(5): 1375-1383.

Carlberg, C. and S. Seuter (2007). "The vitamin D receptor." Dermatol Clin **25**(4): 515-523, viii.

Cheng, J. B., D. L. Motola, D. J. Mangelsdorf and D. W. Russell (2003). "De-orphanization of Cytochrome P450 2R1: A MICROSOMAL VITAMIN D 25-HYDROXYLASE." Journal of Biological Chemistry **278**(39): 38084-38093.

Chertow, B. S., G. R. Baker, H. L. Henry and A. W. Norman (1980). "Effects of vitamin D metabolites on bovine parathyroid hormone release in vitro." Am J Physiol **238**(4): E384-388.

Chick, D. H. (1976). "Study of rickets in Vienna 1919-1922." Med Hist **20**(1): 41-51.

Claes, L., S. Recknagel and A. Ignatius (2012). "Fracture healing under healthy and inflammatory conditions." Nat Rev Rheumatol **8**(3): 133-143.

Dardenne, O., J. Prud'homme, A. Arabian, F. H. Glorieux and R. St-Arnaud (2001). "Targeted inactivation of the 25-hydroxyvitamin D(3)-1(alpha)-hydroxylase gene (CYP27B1) creates an animal model of pseudovitamin D-deficiency rickets." Endocrinology **142**(7): 3135-3141.

Dellinger E, M. S. D. W. M. J. G. M. D. B. A. P. A. (1988). "RIsk of infection after open fracture of the arm or leg." Archives of Surgery **123**(11): 1320-1327.

Deluca, H. F. (2011). Chapter 1 - Historical Overview of Vitamin D. Vitamin D (Third Edition). F. David, J. W. Pike, J. W. P. John S. AdamsA2 - David Feldman and S. A. John. San Diego, Academic Press**:** 3-12.

Delvin, E. E., F. H. Glorieux, P. J. Marie and J. M. Pettifor (1981). "Vitamin D dependency: replacement therapy with calcitriol?" J Pediatr **99**(1): 26-34.

Dusso, A. S., A. J. Brown and E. Slatopolsky (2005). "Vitamin D." Am J Physiol Renal Physiol **289**(1): F8-28.

Eijkman, C. (1897). "Eine Beri Beri-ähnliche Krankheit der Hühner." Archiv für pathologische Anatomie und Physiologie und für klinische Medicin **148**(3): 523-532.

Einhorn, T. A. (1998). "The cell and molecular biology of fracture healing." Clin Orthop Relat Res(355 Suppl): S7-21.

Engstrom, G. W., T. A. Reinhardt and R. L. Horst (1986). "25-Hydroxyvitamin D3-23-hydroxylase, a renal enzyme in several animal species." Arch Biochem Biophys **250**(1): 86-93.

Favus, M. J., M. W. Walling and D. V. Kimberg (1974). "Effects of dietary calcium restriction and chronic thyroparathyroidectomy on the metabolism of (3H)25-hydroxyvitamin D3 and the active transport of calcium by rat intestine." J Clin Invest **53**(4): 1139-1148.

Fraser, D., S. W. Kooh, H. P. Kind, M. F. Holick, Y. Tanaka and H. F. DeLuca (1973). "Pathogenesis of hereditary vitamin-D-dependent rickets. An inborn error of vitamin D metabolism involving defective conversion of 25-hydroxyvitamin D to 1 alpha,25-dihydroxyvitamin D." N Engl J Med **289**(16): 817-822.

Frost, H. M. (1989). "The biology of fracture healing. An overview for clinicians. Part I." Clin Orthop Relat Res(248): 283-293.

Fu, G. K., D. Lin, M. Y. Zhang, D. D. Bikle, C. H. Shackleton, W. L. Miller and A. A. Portale (1997). "Cloning of human 25-hydroxyvitamin D-1 alpha-

hydroxylase and mutations causing vitamin D-dependent rickets type 1." Mol Endocrinol **11**(13): 1961-1970.

Funk, C. (1911). "On the chemical nature of the substance which cures polyneuritis in birds induced by a diet of polished rice." J Physiol **43**(5): 395-400.

Glorieux, F. H., T. Edouard and R. St-Arnaud (2011). Chapter 64 - Pseudo-vitamin D Deficiency. Vitamin D (Third Edition). F. David, J. W. Pike, J. W. P. John S. AdamsA2 - David Feldman and S. A. John. San Diego, Academic Press**:** 1187-1195.

Goltzman, D., D. Miao, D. K. Panda and G. N. Hendy (2004). "Effects of calcium and of the Vitamin D system on skeletal and calcium homeostasis: lessons from genetic models." J Steroid Biochem Mol Biol **89-90**(1-5): 485-489.

Haussler, M. R., D. J. Mangelsdorf, B. S. Komm, C. M. Terpening, K. Yamaoka, E. A. Allegretto, A. R. Baker, J. Shine, D. P. McDonnell, M. Hughes and et al. (1988). "Molecular biology of the vitamin D hormone." Recent Prog Horm Res **44**: 263-305.

Haussler, M. R., G. K. Whitfield, C. A. Haussler, J. C. Hsieh, P. D. Thompson, S. H. Selznick, C. E. Dominguez and P. W. Jurutka (1998). "The nuclear vitamin D receptor: biological and molecular regulatory properties revealed." J Bone Miner Res **13**(3): 325-349.

Heaney, R. P. (2011). Chapter 34 - Vitamin D: Role in the Calcium and Phosphorus Economies. Vitamin D (Third Edition). F. David, J. W. Pike, J. W. P. John S. AdamsA2 - David Feldman and S. A. John. San Diego, Academic Press**:** 607-624.

Hebert, S. C., E. M. Brown and H. W. Harris (1997). "Role of the Ca(2+)-sensing receptor in divalent mineral ion homeostasis." J Exp Biol **200**(Pt 2): 295-302.

Henry, H. L. (2011). "Regulation of vitamin D metabolism." Best Practice & Research Clinical Endocrinology & Metabolism **25**(4): 531-541.

Henry, H. L. and A. W. Norman (1978). "Vitamin D: two dihydroxylated metabolites are required for normal chicken egg hatchability." Science **201**(4358): 835-837.

Hiltunen, A., E. Vuorio and H. T. Aro (1993). "A standardized experimental fracture in the mouse tibia." J Orthop Res **11**(2): 305-312.

Hochberg, Z., D. Tiosano and L. Even (1992). "Calcium therapy for calcitriol-resistant rickets." J Pediatr **121**(5 Pt 1): 803-808.

Hoenderop, J. G., J. P. van Leeuwen, B. C. van der Eerden, F. F. Kersten, A. W. van der Kemp, A. M. Merillat, J. H. Waarsing, B. C. Rossier, V. Vallon, E. Hummler and R. J. Bindels (2003). "Renal Ca2+ wasting, hyperabsorption, and reduced bone thickness in mice lacking TRPV5." J Clin Invest **112**(12): 1906-1914.

Holick, M. F. (2007). "Vitamin D deficiency." N Engl J Med **357**(3): 266-281.

Holick, M. F. (2011). Chapter 2 - Photobiology of Vitamin D. Vitamin D (Third Edition). F. David, J. W. Pike, J. W. P. John S. AdamsA2 - David Feldman and S. A. John. San Diego, Academic Press**:** 13-22.

Holick, M. F. and T. C. Chen (2008). "Vitamin D deficiency: a worldwide problem with health consequences." The American Journal of Clinical Nutrition **87**(4): 1080S-1086S.

Holst, A. and T. Frolich (1907). "Experimental Studies Relating to "Ship-beri-beri" and Scurvy." J Hyg (Lond) **7**(5): 634-671.

Holstein, J. H., R. Matthys, T. Histing, S. C. Becker, M. Fiedler, P. Garcia, C. Meier, T. Pohlemann and M. D. Menger (2009). "Development of a stable closed femoral fracture model in mice." J Surg Res **153**(1): 71-75.

Holstein, J. H., M. D. Menger, U. Culemann, C. Meier and T. Pohlemann (2007). "Development of a locking femur nail for mice." J Biomech **40**(1): 215-219.

Husseini, A. (2011). Bone Formation during Fracture Repair in Mice Deficient for the Cyp24a1 gene. Master of Science in Experimental Surgery, McGill University.

Inaba, M., M. Burgos-Trinidad and H. F. DeLuca (1991). "Characteristics of the 25-hydroxyvitamin D3- and 1,25-dihydroxyvitamin D3-24-hydroxylase(s) from HL-60 cells." Arch Biochem Biophys **284**(2): 257-263.

Ishizuka, S., N. Kurihara, S. V. Reddy, J. Cornish, T. Cundy and G. D. Roodman (2005). "(23S)-25-Dehydro-1{alpha}-hydroxyvitamin D3-26,23-lactone, a vitamin D receptor antagonist that inhibits osteoclast formation and bone resorption in bone marrow cultures from patients with Paget's disease." Endocrinology **146**(4): 2023-2030.

Ishizuka, S. and A. W. Norman (1987). "Metabolic pathways from 1 alpha,25-dihydroxyvitamin D3 to 1 alpha,25-dihydroxyvitamin D3-26,23-lactone. Stereo-retained and stereo-selective lactonization." Journal of Biological Chemistry **262**(15): 7165-7170.

Jarnagin, K., R. Brommage, H. F. DeLuca, S. Yamada and H. Takayama (1983). "1- but not 24-hydroxylation of vitamin D is required for growth and reproduction in rats." American Journal of Physiology - Endocrinology And Metabolism **244**(3): E290-E297.

Kathryn B. Kirkland, M. D., J. P. B. S. N. Briggs, R. N. Sharon L. Trivette, P. William E. Wilkinson and M. D. Daniel J. Sexton (1999). "The Impact of Surgical-Site Infections in the 1990s: Attributable Mortality, Excess Length of Hospitalization, and Extra Costs • " Infection Control and Hospital Epidemiology **20**(11): 725-730.

Khavandgar, Z., C. Poirier, C. J. Clarke, J. Li, N. Wang, M. D. McKee, Y. A. Hannun and M. Murshed (2011). "A cell-autonomous requirement for neutral sphingomyelinase 2 in bone mineralization." J Cell Biol **194**(2): 277-289.

Kolar, P., K. Schmidt-Bleek, H. Schell, T. Gaber, D. Toben, G. Schmidmaier, C. Perka, F. Buttgereit and G. N. Duda (2010). "The early fracture hematoma and its potential role in fracture healing." Tissue Eng Part B Rev **16**(4): 427-434.

Kuriyama, M., J. Fujiyama, R. Kubota, M. Nakagawa and M. Osame (1993). "Correspondence." Metabolism **42**(11): 1497.

Li, Y. C., A. E. Pirro, M. Amling, G. Delling, R. Baron, R. Bronson and M. B. Demay (1997). "Targeted ablation of the vitamin D receptor: an animal model of vitamin D-dependent rickets type II with alopecia." Proc Natl Acad Sci U S A **94**(18): 9831-9835.

Malloy, P. J. and D. Feldman (2010). "Genetic disorders and defects in vitamin d action." Endocrinol Metab Clin North Am **39**(2): 333-346, table of contents.

Malloy, P. J., J. W. Pike and D. Feldman (1999). "The vitamin D receptor and the syndrome of hereditary 1,25-dihydroxyvitamin D-resistant rickets." Endocr Rev **20**(2): 156-188.

Malloy, P. J., D. Tiosano and D. Feldman (2011). Chapter 65 - Hereditary 1,25-Dihydroxyvitamin-D-Resistant Rickets. Vitamin D (Third Edition). F. David, J. W. Pike, J. W. P. John S. AdamsA2 - David Feldman and S. A. John. San Diego, Academic Press**:** 1197-1232.

Masuda, S., M. Kaufmann, V. Byford, M. Gao, R. St-Arnaud, A. Arabian, H. L. Makin, J. C. Knutson, S. Strugnell and G. Jones (2004). "Insights into Vitamin D metabolism using cyp24 over-expression and knockout systems in conjunction with liquid chromatography/mass spectrometry (LC/MS)." J Steroid Biochem Mol Biol **89-90**(1-5): 149-153.

Mazzocca, A., A. Caputo, B. Browner, J. Mast and M. Mendes (2003). Principles of Internal Fixation. Skeletal Trauma. J. B. J. Bruce D. Browner, Alan M Levine, Peter G. Trafton**:** 195-249.

McCollum, E. V., N. Simmonds, J. E. Becker and P. G. Shipley (1922). "Studies On Experimental Rickets: Xxi. An Experimental Demonstration Of The Existence Of A Vitamin Which Promotes Calcium Deposition." Journal of Biological Chemistry **53**(2): 293-312.

McCollum, E. V., N. Simmonds and W. Pitz (1916). "The Relation Of The Unidentified Dietary Factors, The Fat-Soluble A, And Watersoluble B, Of The Diet To The Growthpromoting Properties Of Milk." Journal of Biological Chemistry **27**(1): 33-43.

McKibbin, B. (1978). "The biology of fracture healing in long bones." Journal of Bone & Joint Surgery, British Volume **60-B**(2): 150-162.

Mellanby, E. (1989). "An experimental investigation on rickets. 1919." Nutrition **5**(2): 81-86; discussion 87.

Monkawa, T., T. Yoshida, S. Wakino, T. Shinki, H. Anazawa, H. F. Deluca, T. Suda, M. Hayashi and T. Saruta (1997). "Molecular cloning of cDNA and genomic DNA for human 25-hydroxyvitamin D3 1 alpha-hydroxylase." Biochem Biophys Res Commun **239**(2): 527-533.

Morgan, E. F. and T. A. Einhorn (2009). Chapter 12. Biomechanics of Fracture Healing. Primer on the Metabolic Bone Diseases and Disorders of Mineral Metabolism, John Wiley & Sons, Inc.**:** 65-69.

Naja, R. (2008). The Role of Vitamin D Metabolic Enzymes in Bone Development, McGill University.

Nakamura, T., T. Hirai, K. Suzuki and H. Orimo (1992). "Osteonal remodeling and mechanical properties of the femoral cortex in rabbits treated with 24R,25(OH)2D3." Calcif Tissue Int **50**(1): 74-79.

Nakamura, T., Y. Nagai, H. Yamato, K. Suzuki and H. Orimo (1992). "Regulation of bone turnover and prevention of bone atrophy in ovariectomized beagle dogs by the administration of 24R,25(OH)2D3." Calcif Tissue Int **50**(3): 221-227.

Nakamura, T., K. Suzuki, T. Hirai, T. Kurokawa and H. Orimo (1992). "Increased bone volume and reduced bone turnover in vitamin D-replete rabbits by the administration of 24R,25-dihydroxyvitamin D3." Bone **13**(3): 229-236.

Norman, A. W. (1998). "Receptors for 1α,25(OH)2D3: Past, Present, and Future." Journal Of Bone And Mineral Research **13**(9): 1360-1369.

Norman, A. W., V. Leathers and J. E. Bishop (1983). "Normal egg hatchability requires the simultaneous administration to the hen of 1 alpha,25-dihydroxycholecalciferol and 24R,25-dihydroxycholecalciferol." J Nutr **113**(12): 2505-2515.

Ohyama, Y. and K. Okuda (1991). "Isolation and characterization of a cytochrome P-450 from rat kidney mitochondria that catalyzes the 24-hydroxylation of 25-hydroxyvitamin D3." J Biol Chem **266**(14): 8690-8695.

Omdahl, J. L., H. A. Morris and B. K. May (2002). "Hydroxylase enzymes of the vitamin D pathway: expression, function, and regulation." Annu Rev Nutr **22**: 139-166.

Onyango, I., G. Hjalm, M. Larsson and L. Rask (1999). "Effects of extracellular calcium on the subcellular translocation of bovine parathyroid PKC isozymes." Exp Cell Res **247**(1): 9-16.

Ornoy, A., D. Goodwin, D. Noff and S. Edelstein (1978). "24, 25-dihydroxyvitamin D is a metabolite of vitamin D essential for bone formation." Nature **276**(5687): 517-519.

Pallais, J. C., O. Kifor, Y. B. Chen, D. Slovik and E. M. Brown (2004). "Acquired hypocalciuric hypercalcemia due to autoantibodies against the calcium-sensing receptor." N Engl J Med **351**(4): 362-369.

Panda, D. K., D. Miao, I. Bolivar, J. Li, R. Huo, G. N. Hendy and D. Goltzman (2004). "Inactivation of the 25-hydroxyvitamin D 1alpha-hydroxylase and vitamin D receptor demonstrates independent and interdependent effects of calcium and vitamin D on skeletal and mineral homeostasis." J Biol Chem **279**(16): 16754-16766.

Panda, D. K., D. Miao, M. L. Tremblay, J. Sirois, R. Farookhi, G. N. Hendy and D. Goltzman (2001). "Targeted ablation of the 25-hydroxyvitamin D 1alpha -hydroxylase enzyme: evidence for skeletal, reproductive, and immune dysfunction." Proc Natl Acad Sci U S A **98**(13): 7498-7503.

Pedersen, J. I., Y. Hagenfeldt and I. Bjorkhem (1988). "Assay and properties of 25-hydroxyvitamin D3 23-hydroxylase. Evidence that 23,25-dihydroxyvitamin D3 is a major metabolite in 1,25-dihydroxyvitamin D3-treated or fasted guinea pigs." Biochem J **250**(2): 527-532.

Petkovich, M., C. Helvig and T. Epps (2011). Chapter 80 - CYP24A1 Regulation in Health and Disease. Vitamin D (Third Edition). F. David, J. W. Pike, J.

W. P. John S. AdamsA2 - David Feldman and S. A. John. San Diego, Academic Press**:** 1525-1554.

Prader, A., R. Illig and E. Heierli (1961). "[An unusual form of primary vitamin D-resistant rickets with hypocalcemia and autosomal-dominant hereditary transmission: hereditary pseudo-deficiency rickets]." Helv Paediatr Acta **16**: 452-468.

Rosen, C. J., S. A. Abrams, J. F. Aloia, P. M. Brannon, S. K. Clinton, R. A. Durazo-Arvizu, J. C. Gallagher, R. L. Gallo, G. Jones, C. S. Kovacs, J. E. Manson, S. T. Mayne, A. C. Ross, S. A. Shapses and C. L. Taylor (2012). "IOM committee members respond to Endocrine Society vitamin D guideline." J Clin Endocrinol Metab **97**(4): 1146-1152.

Ross, A. C., J. E. Manson, S. A. Abrams, J. F. Aloia, P. M. Brannon, S. K. Clinton, R. A. Durazo-Arvizu, J. C. Gallagher, R. L. Gallo, G. Jones, C. S. Kovacs, S. T. Mayne, C. J. Rosen and S. A. Shapses (2011). "The 2011 report on dietary reference intakes for calcium and vitamin D from the Institute of Medicine: what clinicians need to know." J Clin Endocrinol Metab **96**(1): 53-58.

Sakaki, T., N. Sawada, K. Komai, S. Shiozawa, S. Yamada, K. Yamamoto, Y. Ohyama and K. Inouye (2000). "Dual metabolic pathway of 25-hydroxyvitamin D3 catalyzed by human CYP24." Eur J Biochem **267**(20): 6158-6165.

Sakaki, T., N. Sawada, Y. Nonaka, Y. Ohyama and K. Inouye (1999). "Metabolic studies using recombinant escherichia coli cells producing rat mitochondrial CYP24 CYP24 can convert 1alpha,25-dihydroxyvitamin D3 to calcitroic acid." Eur J Biochem **262**(1): 43-48.

Schlingmann, K. P., M. Kaufmann, S. Weber, A. Irwin, C. Goos, U. John, J. Misselwitz, G. Klaus, E. Kuwertz-Broking, H. Fehrenbach, A. M. Wingen, T. Guran, J. G. Hoenderop, R. J. Bindels, D. E. Prosser, G. Jones and M. Konrad (2011). "Mutations in CYP24A1 and idiopathic infantile hypercalcemia." N Engl J Med **365**(5): 410-421.

Schwartz, Z. V. I. and B. Boyan (1988). "The Effects of Vitamin D Metabolites on Phospholipase A2 Activity of Growth Zone and Resting Zone Cartilage Cells in Vitro." Endocrinology **122**(5): 2191-2198.

Schwartz, Z. V. I., D. L. Schlader, L. D. Swain and B. D. Boyan (1988). "Direct Effects of 1,25-Dihydroxyvitamin D3 and 24,25-Dihydroxyvitamin D3 on Growth Zone and Resting Zone Chondrocyte Membrane Alkaline Phosphatase and Phospholipase-A2 Specific Activities." Endocrinology **123**(6): 2878-2884.

Seo, E. G., T. A. Einhorn and A. W. Norman (1997). "24R,25-dihydroxyvitamin D3: an essential vitamin D3 metabolite for both normal bone integrity and healing of tibial fracture in chicks." Endocrinology **138**(9): 3864-3872.

Seo, E. G., A. Kato and A. W. Norman (1996). "Evidence for a 24R,25(OH)2-vitamin D3 receptor/binding protein in a membrane fraction isolated from a chick tibial fracture-healing callus." Biochem Biophys Res Commun **225**(1): 203-208.

Seo, E. G. and A. W. Norman (1997). "Three-fold induction of renal 25-hydroxyvitamin D3-24-hydroxylase activity and increased serum 24,25-dihydroxyvitamin D3 levels are correlated with the healing process after chick tibial fracture." J Bone Miner Res **12**(4): 598-606.

Shinki, T., H. Shimada, S. Wakino, H. Anazawa, M. Hayashi, T. Saruta, H. F. DeLuca and T. Suda (1997). "Cloning and expression of rat 25-hydroxyvitamin D3-1alpha-hydroxylase cDNA." Proc Natl Acad Sci U S A **94**(24): 12920-12925.

Skorija, K., M. Cox, J. M. Sisk, D. R. Dowd, P. N. MacDonald, C. C. Thompson and M. B. Demay (2005). "Ligand-independent actions of the vitamin D receptor maintain hair follicle homeostasis." Mol Endocrinol **19**(4): 855-862.

St-Arnaud, R. (1999). "Targeted inactivation of vitamin D hydroxylases in mice." Bone **25**(1): 127-129.

St-Arnaud, R. (2010). "CYP24A1-deficient mice as a tool to uncover a biological activity for vitamin D metabolites hydroxylated at position 24." J Steroid Biochem Mol Biol **121**(1-2): 254-256.

St-Arnaud, R. (2011). Chapter 4 - CYP24A1: Structure, Function, and Physiological Role. Vitamin D (Third Edition). F. David, J. W. Pike, J. W. P. John S. AdamsA2 - David Feldman and S. A. John. San Diego, Academic Press**:** 43-56.

St-Arnaud, R., A. Arabian, R. Travers, F. Barletta, M. Raval-Pandya, K. Chapin, J. Depovere, C. Mathieu, S. Christakos, M. B. Demay and F. H. Glorieux (2000). "Deficient mineralization of intramembranous bone in vitamin D-24-hydroxylase-ablated mice is due to elevated 1,25-dihydroxyvitamin D and not to the absence of 24,25-dihydroxyvitamin D." Endocrinology **141**(7): 2658-2666.

St-Arnaud, R. and M. B. Demay (2012). Chapter 8 - Vitamin D Biology. Pediatric Bone (Second Edition). H. G. Francis, M. P. John, J. M. P. Harald JüppnerA2 - Francis H. Glorieux and J. Harald. San Diego, Academic Press**:** 163-187.

St-Arnaud, R., S. Messerlian, J. M. Moir, J. L. Omdahl and F. H. Glorieux (1997). "The 25-hydroxyvitamin D 1-alpha-hydroxylase gene maps to the pseudovitamin D-deficiency rickets (PDDR) disease locus." J Bone Miner Res **12**(10): 1552-1559.

Steenbock, H., A. Black, C. A. H. With the cooperation of Mariana T. Nelson and M. R. Blanche (1925). "Fat-Soluble Vitamins: Xxiii. The Induction Of Growth-Promoting And Calcifying Properties In Fats And Their Unsaponifiable Constituents By Exposure To Light." Journal of Biological Chemistry **64**(2): 263-298.

Stoffel, W., B. Jenke, B. Block, M. Zumbansen and J. Koebke (2005). "Neutral sphingomyelinase 2 (smpd3) in the control of postnatal growth and development." Proc Natl Acad Sci U S A **102**(12): 4554-4559.

Stoffel, W., B. Jenke, B. Holz, E. Binczek, R. H. Gunter, J. Knifka, J. Koebke and A. Niehoff (2007). "Neutral sphingomyelinase (SMPD3) deficiency causes a novel form of chondrodysplasia and dwarfism that is rescued by

Col2A1-driven smpd3 transgene expression." Am J Pathol **171**(1): 153-161.

Takeyama, K., S. Kitanaka, T. Sato, M. Kobori, J. Yanagisawa and S. Kato (1997). "25-Hydroxyvitamin D3 1alpha-hydroxylase and vitamin D synthesis." Science **277**(5333): 1827-1830.

Tanaka, Y., H. F. DeLuca, Y. Kobayashi, T. Taguchi, N. Ikekawa and M. Morisaki (1979). "Biological activity of 24,24-difluoro-25-hydroxyvitamin D3. Effect of blocking of 24-hydroxylation on the functions of vitamin D." J Biol Chem **254**(15): 7163-7167.

Thacher, T. D. and B. L. Clarke (2011). "Vitamin D insufficiency." Mayo Clin Proc **86**(1): 50-60.

Tiosano, D., Y. Weisman and Z. Hochberg (2001). "The role of the vitamin D receptor in regulating vitamin D metabolism: a study of vitamin D-dependent rickets, type II." J Clin Endocrinol Metab **86**(5): 1908-1912.

Toell, A., M. M. Gonzalez, D. Ruf, A. Steinmeyer, S. Ishizuka and C. Carlberg (2001). "Different molecular mechanisms of vitamin D(3) receptor antagonists." Mol Pharmacol **59**(6): 1478-1485.

Turner, C. H. and D. B. Burr (1993). "Basic biomechanical measurements of bone: a tutorial." Bone **14**(4): 595-608.

Weisman, Y., I. Bab, D. Gazit, Z. Spirer, M. Jaffe and Z. Hochberg (1987). "Long-term intracaval calcium infusion therapy in end-organ resistance to 1,25-dihydroxyvitamin D." Am J Med **83**(5): 984-990.

White, A. A., 3rd, M. M. Panjabi and W. O. Southwick (1977). "The four biomechanical stages of fracture repair." J Bone Joint Surg Am **59**(2): 188-192.

Windaus, A., F. Schenck and F. T. Werder (1936). Über das antirachitisch wirksame Bestrahlungsprodukt ans 7-Dehydro-cholesterin. Hoppe-Seyler´s Zeitschrift für physiologische Chemie. **241:** 100.

Wray, J. B. (1964). "Acute Changes in Femoral Arterial Blood Flow after Closed Tibial Fracture in Dogs." J Bone Joint Surg Am **46**: 1262-1268.

Xu, H., L. Bai, J. F. Collins and F. K. Ghishan (2002). "Age-dependent regulation of rat intestinal type IIb sodium-phosphate cotransporter by 1,25-(OH)(2) vitamin D(3)." Am J Physiol Cell Physiol **282**(3): C487-493.

Yamagata, M., A. Kimoto, T. Michigami, M. Nakayama and K. Ozono (2001). "Hydroxylases involved in vitamin D metabolism are differentially expressed in murine embryonic kidney: application of whole mount in situ hybridization." Endocrinology **142**(7): 3223-3230.

Yamashita-Sugahara, Y., Y. Tokuzawa, Y. Nakachi, Y. Kanesaki-Yatsuka, M. Matsumoto, Y. Mizuno and Y. Okazaki (2013). "Fam57b (Family with Sequence Similarity 57, Member B), a Novel Peroxisome Proliferator-activated Receptor γ Target Gene That Regulates Adipogenesis through Ceramide Synthesis." Journal of Biological Chemistry **288**(7): 4522-4537.

Yamate, T., H. Tanaka, Y. Nagai, H. Yamato, N. Taniguchi, T. Nakamura and Y. Seino (1994). "Bone-forming ability of 24R,25-dihydroxyvitamin D3 in the hypophosphatemic mouse." J Bone Miner Res **9**(12): 1967-1974.

Yoshizawa, T., Y. Handa, Y. Uematsu, S. Takeda, K. Sekine, Y. Yoshihara, T. Kawakami, K. Arioka, H. Sato, Y. Uchiyama, S. Masushige, A. Fukamizu, T. Matsumoto and S. Kato (1997). "Mice lacking the vitamin D receptor exhibit impaired bone formation, uterine hypoplasia and growth retardation after weaning." Nat Genet **16**(4): 391-396.